

# Physical Layer Deception based on Semantic Distortion

Wenwen Chen, Bin Han, Yao Zhu, Anke Schmeink, Giuseppe Caire, and Hans D. Schotten

**Physical layer deception (PLD) is a framework we previously introduced that integrates physical layer security (PLS) with deception techniques, enabling proactive countermeasures against eavesdropping rather than relying solely on passive defense. We extend this framework to a semantic communication model and conduct a theoretical analysis using semantic distortion as the performance metric. In this work, we further investigate the receiver's selection of decryption strategies and the transmitter's optimization of encryption strategies. By anticipating the decryption strategy likely to be employed by the legitimate receiver and eavesdropper, the transmitter can optimize resource allocation and encryption parameters, thereby maximizing the semantic distortion at the eavesdropper while maintaining a low level of semantic distortion for the legitimate receiver. We present a rigorous analysis of the resulting optimization problem, propose an efficient optimization algorithm, and derive closed-form optimal solutions for multiple scenarios. Finally, we corroborate the theoretical findings with numerical simulations, which also confirm the practicality of the proposed algorithm.**

**Index Terms**—Physical layer security, semantic communication, semantic security, finite blocklength codes.

## I. INTRODUCTION

Physical layer security (PLS) is an emerging approach for securing transmitted data in wireless communication. Compared with cryptographic methods, PLS leverages the inherent randomness of the communication medium and does not involve high computational complexity or costly key management, which makes it more suitable for the new wireless technologies such as Internet of Things (IoT), massive machine-type communication (mMTC), ultra-reliable low-latency communication (URLLC) 5G-Tactile Internet, etc [1]. PLS technologies can effectively counter both passive and active attacks, including eavesdropping, impersonation, and message falsification [2]. It can serve as an additional layer of protection to strengthen the security of the radio access network (RAN) with lightweight mechanisms, and can make use of both contextual information and the semantics of the transmitted data [3].

Although recent advancements in PLS have improved passive security, a significant imbalance persists: eavesdroppers can always attempt to intercept communication with minimal risk of detection and require far less effort [4] than the considerable resources and precautions required by the legitimate users to protect the data [5] [6]. This imbalance highlights the need to incorporate active defense strategies—such as deception technologies—into the wireless security framework.

W. Chen, B. Han, and H. D. Schotten are with RPTU Kaiserslautern-Landau, Germany. Y. Zhu and A. Schmeink are with RWTH Aachen University, Germany. G. Caire is with Technical University of Berlin, Germany. H. D. Schotten is with the German Research Center for Artificial Intelligence (DFKI), Germany. B. Han (bin.han@rptu.de) is the corresponding author.

These technologies aim to mislead and divert potential eavesdroppers by generating false data or environments, thereby safeguarding real information. In addition, they can provoke eavesdroppers into exposing their presence, providing a proactive method of enhancing security [7].

To mitigate this imbalance, we introduced the novel physical layer deception (PLD) framework in our previous work [8] [9]. This PLD framework integrates PLS with deception techniques to actively defend against eavesdroppers by misleading them with falsified information, while preserving normal communication over the legitimate channel. In our subsequent work [10], to facilitate the design of the encryptor and improve compatibility with conventional wireless communication protocols, we replaced the non-orthogonal multiplexing (NOM) modulation scheme with orthogonal frequency-division multiplexing (OFDM), significantly simplifying the decryption process. Compared to traditional PLS approaches, our proposed method achieves a high deception rate without compromising security or reliability.

However, previous studies still have limitations, as optimization objectives were restricted to the deception rate and leakage-failure probability, making the approach less generalizable across different applications. Moreover, previous studies have considered only the transmitter's encryption strategy, without taking into account the decryption strategies of the legitimate receiver and the eavesdropper. Therefore, in [11] we employ a semantic model to interpret the PLD framework and introduce a more general metric, namely semantic distortion, to evaluate both the reliability and security of communication. This semantic model does not depend on any specific coding or modulation scheme, making it a more general and flexible system implementation. Moreover, based on the semantic model, we also derive the optimal decryption strategy at the receiver to minimize the semantic distortion.

In this work, we optimize the transmitter's resource allocation scheme and encryptor's activation rate based on the decryption strategies of the eavesdropper and the intended receiver. The goal is to ensure secure and reliable communication for the legitimate user while maximizing the semantic distortion experienced by the eavesdropper. Our contributions are summarized as follows:

- 1) We conduct a theoretical analysis of the optimization problem and prove the convexity of the objective function under three different decryption strategies adopted by the eavesdropper. We further categorize the problem into nine cases and derive analytical solutions for the optimal values.
- 2) We propose an optimization algorithm that allows the transmitter to efficiently determine the optimal encryption rate and coding rate after predicting the decryption

strategies of both eavesdropper and intended receiver.

3) We perform simulation experiments under various parameter settings based on the proposed algorithm and observe that the strategy choices of eavesdropper and legitimate receiver exhibit a periodic pattern.

In Section II, we briefly review the related literature. Section III introduces the PLD framework, the decryption strategies at the receiver, and the corresponding performance metric. Section III presents the analysis of the optimization problem and derives the analytical expressions for the optimal solution. In Section IV, we conduct simulation experiments to validate the theoretical analysis and examine the tendencies in the receiver's strategy selection under different parameter settings.

## II. RELATED WORKS

Modern security theory traces back to *Shannon*'s foundational work on secrecy systems, which proved that perfect secrecy can be achieved through cryptographic methods assuming noiseless channels and shared secret keys [12]. Unlike *Shannon*'s secrecy model, *Wyner* [13] introduced the wiretap channel in 1975, showing that perfect secrecy could be achieved at the physical layer without relying on secret keys if the eavesdropping channel is a degraded version of the legitimate channel. This work also proved that the secrecy capacity of a discrete memoryless channel is defined as the maximum difference between the mutual information of the legitimate channel and that of the eavesdropping channel. Building on *Wyner*'s pioneering work, researchers have investigated the achievable secrecy capacity from an information-theoretic perspective, considering different channel models and communication scenarios. *Csiszár* and *Körner* extended the degraded wiretap channel model to a broadcast channel with confidential messages and analyzed the secrecy capacity for a more general, non-degraded wiretap channel [14]. The fundamental issues of secure channel capacity were also studied over Gaussian channel [15], fading channels [16], multi-input multi-output (MIMO) channel [17], single-input multiple-output (SIMO) channel [18], multiple-input single-output (MISO) channel [19], broadcast channel [20], multiple-access channel [21], interference channel [22], relay channel [23], etc. In addition, some studies have focused on the secrecy capacity under different channel state information (CSI) assumptions about the availability of eavesdropper's CSI, such as under full CSI [24], imperfect CSI [25], or no CSI [26]. The transmitter can also combine different techniques to enhance security, such as adaptive coding and modulation, optimal power allocation, adaptive scheduling and resource allocation, partial pre-equalization, pre-coding, antenna selection, etc [27].

In order to study transmission performance in the finite blocklength (FBL) regime, the seminal work [28] derived a tight bound with a closed-form expression for the decoding error probability. This expression and its first-order approximation have been extensively used to analyze FBL performance, particularly in the context of URLLC [29]–[31]. The authors in [32] derived new achievability and converse bounds that are uniformly tighter than previous bounds, thereby providing

the tightest bounds on the second-order coding rate for both discrete memoryless and Gaussian wiretap channels. Based on this foundation, numerous studies have been conducted to further improve PLS performance in the FBL regime. The authors in [33] jointly optimized the precoder and artificial noise to maximize the secrecy rate under the covertness constraint. In [34], the trade-off between reliability and security is investigated, demonstrating that joint secure-reliability performance can be improved through appropriate allocation of transmission resources. The authors in [35] investigated the reliability-security tradeoff by defining a new metric, leakage-failure probability, which jointly characterizes both reliability and security performances for short-packet transmissions.

In information security, the concept of deception was initially introduced and demonstrated by *Mitnick*'s social engineering tactics. Subsequently, *Cheswick* [36] and *Stoll* [37] extended this idea to defensive mechanisms, introducing the notion of *honeypots*, which later evolved into a wider range of *deception technologies* [38]. The fundamental idea of deception technologies is to mislead and divert attackers with fake data that closely resembles real confidential information, thereby safeguarding authentic information. These tools can also provoke attackers into exposing their presence, providing a proactive method for preserving security. Over the past 30 years, deception techniques have seen significant development and have been widely implemented across various layers of information systems, including the network, system, application, and data layers. Numerous approaches have been introduced to mitigate, prevent, or detect cyber attacks. For a comprehensive review on the state-of-the-art of deception technologies, readers are referred to [38]–[40]. However, deception technologies at the physical layer remain in the early stages of development. The authors in [41] achieve this by exploiting multi-antenna transmission and channel differences to confuse the eavesdropper with the “fake” but meaningful messages and guiding eavesdroppers into trap regions. In [42], an adversarial defense embedded waveform design method based on generative adversarial network (GAN) is proposed to reduce the bit error rate loss for legitimate users and set up the defense trap for the eavesdropper. In [43], the authors proposed a defensive deceptive communication waveform, which embeds sophisticated camouflage or inducement features into the transmitted signals to mislead the direction cognition and alignment of eavesdroppers.

## III. PROBLEM SETUP

### A. System Model

The principle of PLD framework is shown in Fig.1, where a typical wireless eavesdropping scenario is considered. The transmitter *Alice* sends encrypted messages to the legitimate user *Bob* over the legitimate channel  $h_{Bob}$ , while an eavesdropper *Eve* listens to *Alice* over the eavesdropping channel  $h_{Eve}$ . By employing proper beamforming, *Alice* can ensure that  $h_{Bob}$  remains statistically better than  $h_{Eve}$ , thereby enabling the use of PLS methods.

At the transmitter, *Alice* activates deceptive ciphering with probability  $\alpha$ . With the randomly selected key  $k \in \mathbb{K}$ , the

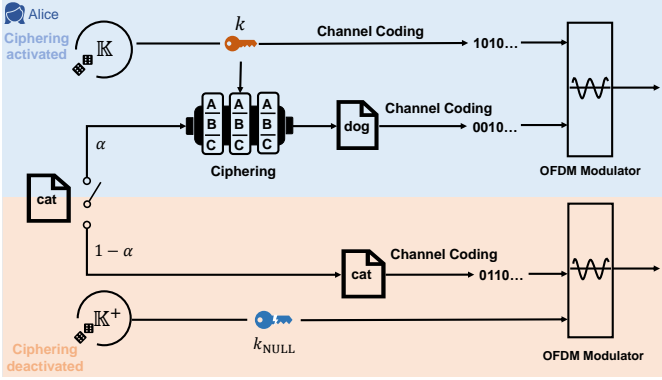


Fig. 1: System model of PLD at the transmitter side

plaintext  $p \in \mathbb{S}$  is encrypted into ciphertext  $m \in \mathbb{S}$ . We define the encryption process as:

$$m = f_k(p) \in \mathbb{S}, \quad \forall (p, k) \in (\mathbb{S} \times \mathbb{K}). \quad (1)$$

On the other hand, once the chosen key  $k$  is known, the plaintext  $p$  can be uniquely decrypted from the ciphertext  $m$ :

$$p = f_k^{-1}(m). \quad (2)$$

When the cipherer is deactivated, *Alice* transmits the plaintext without encryption, i.e.,  $m = p$ . To prevent *Eve* from inferring the status of the cipherer based on the received signal power, *Alice* simultaneously transmits a litter sequence  $k_{\text{NULL}}$ .

It is important to emphasize that the codebook  $\mathbb{S}$  must be carefully designed such that both the plaintext and the ciphertext are valid elements within it. The encryption process effectively maps the original plaintext to another legitimate message in the same codebook. This design serves as a fundamental prerequisite for achieving deception. When *Eve* fails to decode the key and consequently assumes that *Alice* is transmitting a random sequence, *Eve* will naturally interpret the ciphertext as the original message. Since both the plaintext and ciphertext belong to the same codebook and each carries plausible semantic meaning, *Eve* has no reason to question the authenticity of the received message.

We consider a worst-case scenario in which the eavesdropper has full knowledge of the PLD mechanisms, and the modulation and channel coding schemes are publicly known and shared among *Alice*, *Bob*, and *Eve*. This assumption represents a specific type of real-world security threat—such as a breached database or a malicious insider—where the eavesdropper possesses the same level of system knowledge as the legitimate receiver.

At the receiver side, *Bob* and *Eve* decode both the ciphertext and the key simultaneously, as illustrated in Fig. 2. After channel decoding, if the ciphertext cannot be successfully decoded, the receiver simply discards the information. If the ciphertext is successfully decoded, the receiver's subsequent action depends on the decoding outcome of the key. When the key is also correctly decoded, the corresponding plaintext  $\hat{p}$  can be recovered from  $\hat{m}$  and  $\hat{k}$ . Otherwise, if the key decoding fails, the receiver may adopt one of three possible decryption strategies:

1) *Perception*: The receiver assumes that the deceptive ciphering was deactivated, i.e., no valid key was transmitted. Thus, it interprets the decoded ciphertext as an unencrypted plaintext, i.e.,  $\hat{m} = \hat{p}$ . This approach is also the default choice used by deterministic decryption schemes.

2) *Dropping*: The receiver cannot determine whether the failure of decoding is due to poor channel quality preventing the decoding of a valid key, or because *Alice* transmitted  $k_{\text{NULL}}$ . Thus, the receiver simply drops the received message  $\hat{m}$ , treating it as  $\hat{p} = s_{\text{NULL}}$ .

3) *Exclusion*: The receiver assumes that a valid key was transmitted but not correctly decoded, which means that the ciphertext is not equal to the plaintext. Thus, the receiver should select another codeword  $\hat{p} \neq \hat{m}$  for  $\hat{p} \in \mathbb{S}$ . We assume that  $\Pr(p) = \frac{1}{|\mathbb{S}|}$  for all  $p \in \mathbb{S}$ , where  $\mathbb{S}$  is the codebook cardinality. In this case, the optimal strategy to select  $\hat{p}$  shall follow the principle of maximum likelihood:

$$f_{\hat{k}}^{-1}(\hat{m}) = \arg \max_{p \in \mathbb{S} \setminus \{\hat{m}\}} \Pr(p). \quad (3)$$

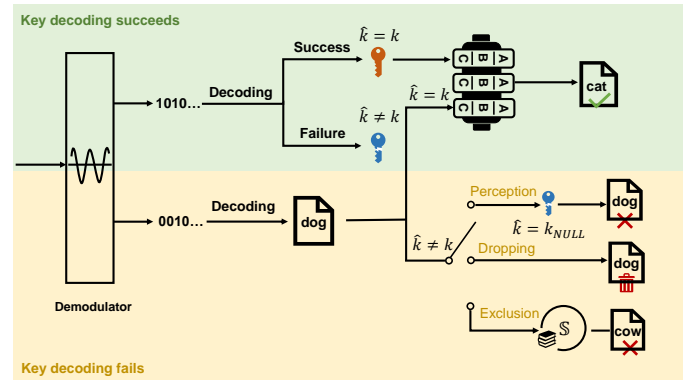


Fig. 2: Decryptor model at the receiver side

It shall be noted that the three decryption strategies are applicable to both *Eve* and *Bob*. In the subsequent analysis, both *Bob* and *Eve* perform decryption based on this mechanism. Due to the superior conditions of the legitimate channel, *Bob* is highly likely to correctly decode both the ciphertext and the key, thereby recovering the intended plaintext. In contrast, *Eve* is less likely to decode the key successfully and is consequently more inclined to employ one of the three decryption strategies. Moreover, it is worth noting that in real-world deployment, if *Alice* is properly configured to encode both the message and the key with adequate redundancy and transmit them at sufficient power levels, the likelihood of mistaking one valid codeword for another is assumed to be negligible compared to the probability of a decoding failure. Therefore, in the following analysis, we only consider the case of *Erasure* for decoding error, where bit errors exceed the correction capability but remain within the detection capability.

For the receiver, whether it mistakenly believes that *Alice* did not send a valid key and directly treats the ciphertext as the plaintext, or randomly selects a codeword from the remaining entries in the codebook as the plaintext, it ends up obtaining incorrect information in either case. Therefore, we can design

special codebooks so that, after decrypting false information, deception will lead to a penalty and *Eve* may either stop eavesdropping or even reveal herself, thereby enabling active defense against the eavesdropper.

### B. Performance Metrics

This communication model employing PLD can be explained using the theory of semantic communication. The plaintext  $p \in \mathbb{S}$  can be considered as a meaning, and the ciphertext  $m \in \mathbb{S}$  can be considered as a message. For each encryption process, *Alice* essentially encodes the meaning(plaintext)  $p \in \mathbb{S}$  into a message(ciphertext)  $m \in \mathbb{S}$  with the randomly selected key  $k \in \mathbb{K}$ . Thus, the encryptor of the PLD framework can be considered as a semantic encoder [44] and we define this encoder as  $u_k$ , which is depicted in Fig. 3. The  $\mathbb{S}$  and  $\mathbb{K}$  represent the set of feasible plaintext codewords and the keys, respectively.

On the other hand, when the deceptive ciphering is deactivated, *Alice* sends the unciphered plaintext  $p \in \mathbb{S}$  together with a litter sequence  $k_{\text{NULL}}$ . Hence, we define  $\mathbb{K}^+ = \mathbb{K} \cup \{k_{\text{NULL}}\}$  to integrate both cases into a unified model, where each message(ciphertext) is semantically encoded by  $u_k$  with  $k \in \mathbb{K}^+$ . In particular, we have  $u_{k_{\text{NULL}}}(p) = p$  for all  $p \in \mathbb{S}$ .

Correspondingly, at the receiver side, the semantic decoder  $v_{\hat{k}}$  uses the received key  $\hat{k} \in \mathbb{K}^+$  to decode the channel-decoded message(ciphertext)  $\hat{m} \in \mathbb{S}^+$  into the meaning(plaintext)  $\hat{p}$ , where  $\mathbb{S}^+ = \mathbb{S} \cup \{s_{\text{NULL}}\}$  and  $s_{\text{NULL}}$  denotes the decoding error flag.

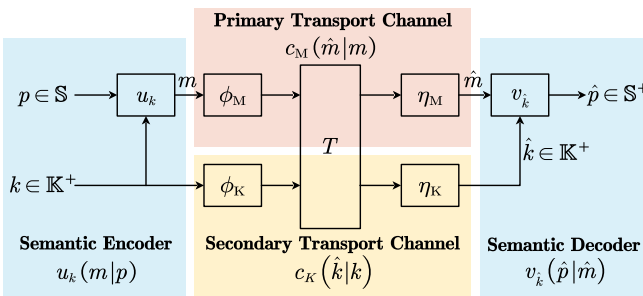


Fig. 3: Dual-channel model of PLD

To distinguish between the channel models of the ciphertext and the key, we define the transmission channel for the ciphertext as the *primary transport channel*, and the transmission channel for the key as the *secondary transport channel*. In the *primary transport channel*, the encrypted meaning(ciphertext)  $m$  first passes through the channel encoder  $\phi_M$ , then is transmitted over the physical channel  $T$ , and finally decoded at the receiver by the channel decoder  $\eta_M$  to obtain  $\hat{m}$ . As mentioned above, with appropriate channel coding and error detection, the occurrence of the case *confusion*—namely, decoding one codeword into another valid codeword—can be regarded as negligible. Therefore, the *primary transport channel* can be modeled as an erasure channel, as illustrated in Fig. 4.

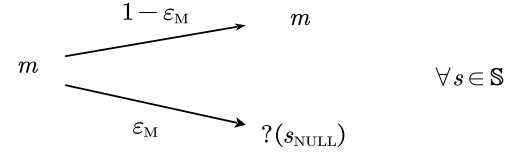


Fig. 4: Model of the primary transport channel

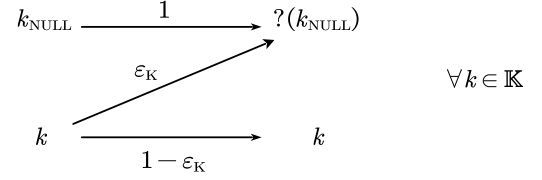


Fig. 5: Model of the secondary transport channel

We can easily obtain the conditional probability density function (PDF) of the *primary transport channel*:

$$c_M(\hat{m}|m) = \begin{cases} 1 - \varepsilon_M, & \hat{m} = m \\ \varepsilon_M, & \hat{m} = s_{\text{NULL}} \\ 0, & \text{otherwise} \end{cases} \quad (4)$$

$$= (1 - \varepsilon_M)\delta(\hat{m} - m) + \varepsilon_M\delta(\hat{m} - s_{\text{NULL}})$$

For the secondary transport channel, since litter sequences are transmitted randomly, the channel model takes on a Z-shape, as shown in Fig. 5. The conditional PDF of the *secondary transport channel* can be formulated as:

$$c_K(\hat{k}|k) = \begin{cases} 1 - \varepsilon_K, & \hat{k} = k, k \in \mathbb{K} \\ \varepsilon_K, & \hat{k} = k_{\text{NULL}} \neq k, k \in \mathbb{K} \\ 1, & \hat{k} = k = k_{\text{NULL}} \\ 0, & \text{otherwise} \end{cases} \quad (5)$$

$$= [(1 - \varepsilon_K)\delta(\hat{k} - k) + \varepsilon_K\delta(\hat{k} - k_{\text{NULL}})] \cdot [1 - \delta(k - k_{\text{NULL}})] + \delta(\hat{k} - k_{\text{NULL}}).$$

Next, we introduce semantic distortion to evaluate the performance of semantic encoding and decoding, and define the semantic distortion between meaning  $p_1 \in \mathbb{S}^+$  and  $p_2 \in \mathbb{S}^+$  as  $d(p_1, p_2)$ . Thus,  $d(p, p) = 0, p \in \mathbb{S}^+$  always holds.

From the expressions of the two transport channels, together with the semantic encoder and decoder, we can derive the expression for the conditional PDF of the whole semantic communication channel:

$$\psi(\hat{p}|p) = \sum_{p, \hat{p}, k, \hat{k}} \Pr(k) u_k(m|p) c_M(\hat{m}|m) c_K(\hat{k}|k) v_{\hat{k}}(\hat{p}|\hat{m}), \quad (6)$$

and the average semantic distortion achieved by *Bob* can be derived as:

$$D = \sum_{p, \hat{p}} \Pr(p) \psi(\hat{p}|p) d(p, \hat{p}). \quad (7)$$

It is worth noting that once the key  $k$  is given, the semantic encoder and decoder can be described deterministically as

$m = f_k(p)$  and  $\hat{p} = f_k^{-1}(\hat{m})$ , respectively. Thus, we can obtain the expression of the semantic encoder and decoder:

$$u_k(m|p) = \begin{cases} 1, & m = f_k(p), \\ 0, & \text{otherwise,} \end{cases} \quad (8)$$

$$v_k(\hat{p}|\hat{m}) = \begin{cases} 1, & \hat{p} = f_{\hat{k}}^{-1}(\hat{m}), \\ 0, & \text{otherwise,} \end{cases} \quad (9)$$

After taking into account the primary transport model and decode failure case, and introducing a parameter  $\alpha \in [0, 1]$  to represent the probability of activating encryption, we can reformulate (7) as:

$$D = \varepsilon_M d(p, s_{\text{NULL}}) + (1 - \varepsilon_M) \varepsilon_K \sum_p \Pr(p) \sum_{k \in \mathbb{K}} \Pr(k) d(p, f_k(p)). \quad (10)$$

In the above equation, once the codebook is designed, the values of  $d(p, s_{\text{NULL}})$  and  $d(p, f_k(p))$  become fixed and can thus be regarded as constants in the optimization problem. Accordingly, we define  $d(p, s_{\text{NULL}}) = D_{\text{loss}}$ ,  $d(p, f_k(p)) = D_{\text{conf}}$ , which denote the distortion caused by message loss and the distortion caused by confusion. Consequently, (10) can be simplified into:

$$D_i = \varepsilon_{i,M} D_{\text{loss}} + \alpha(1 - \varepsilon_{i,M}) \varepsilon_{i,K} D_{\text{conf}}, \quad (11)$$

where  $i \in \{\text{Bob}, \text{Eve}\}$ .

### C. Decryptor Model

According to the PLD framework, the deception only occurs when the receiver fails to decode the key, which is quantified by  $D_{\text{conf}}$ . Thus, the receiver must also design a decryption scheme to reduce  $D_{\text{conf}}$ . When obtaining a  $\hat{k} = k_{\text{NULL}}$ , the receiver may choose one of the following three schemes: *Perception*, *Dropping*, and *Dropping*, which is also depicted in Fig. 2. For convenience of discussion, we assume  $\Pr(p) = \frac{1}{S}$ , where  $S$  denotes the codebook cardinality. In this case, we assume the probabilities of selecting each of the three options are given by  $(\beta_1, \beta_2, \beta_3)$ . Thus, we can obtain the expression of a stochastic semantic decoder:

$$\tilde{v}_{\hat{k}}(\hat{p}|\hat{m}) = \begin{cases} 1, & \hat{p} = f_{\hat{k}}^{-1}(\hat{m}), \hat{k} \neq k_{\text{NULL}} \\ \beta_1, & \hat{p} = \hat{m}, \hat{k} = k_{\text{NULL}} \\ \beta_2, & \hat{p} = m_{\text{NULL}}, \hat{k} = k_{\text{NULL}} \\ \frac{\beta_3}{S-1}, & \hat{p} \in \mathbb{S} \setminus \{\hat{m}\}, \hat{k} = k_{\text{NULL}} \\ 0, & \text{otherwise} \end{cases} \quad (12)$$

The distortion based on an opportunistic decryptor can be presented as:

$$\tilde{D}_i = \varepsilon_{i,M} D_{\text{loss}} + (1 - \varepsilon_{i,M}) \left\{ \begin{array}{l} \beta_1 \underbrace{\varepsilon_{i,K} \alpha D_{\text{conf}}}_{\Delta_1} \\ + \beta_2 \underbrace{[\varepsilon_{i,K} \alpha + (1 - \alpha)] D_{\text{loss}}}_{\Delta_2} \\ + \beta_3 \underbrace{\left[ \varepsilon_{i,K} \frac{\alpha(S-2)}{S-1} D_{\text{conf}} + (1 - \alpha) D_{\text{conf}} \right]}_{\Delta_3} \end{array} \right\} \quad (13)$$

For analytical convenience and clearer interpretation, we introduce a coefficient  $\beta_k \in \{0, 1\}$  to weight the distortion term associated with each of the three decryption strategies. A value of  $\beta_k = 1$  indicates that the receiver adopts the  $k$ -th strategy. Meanwhile, we define  $\Delta_k$  as the distortion value incurred when the  $k$ -th decryption strategy is selected.

At the receiver end, the packet error rates  $\varepsilon_{i,M}$  and  $\varepsilon_{i,K}$  for  $i \in \{\text{Bob}, \text{Eve}\}$  can be determined given certain channel conditions and radio resource allocation scheme. Thus, both *Bob* and *Eve* can select the optimal scheme  $(\beta_1^i, \beta_2^i, \beta_3^i)$  to minimize the distortion  $\tilde{D}_i$ . This optimization problem can be formulated as:

$$\begin{aligned} & \text{minimize}_{\beta_1^i, \beta_2^i, \beta_3^i} \quad \tilde{D}_i = \tilde{D}_i(\varepsilon_{i,M}, \varepsilon_{i,K}) \end{aligned} \quad (14a)$$

$$\text{subject to} \quad \beta_1^i + \beta_2^i + \beta_3^i = 1. \quad (14b)$$

This optimization problem is a linear programming problem and can be easily solved by assigning  $\beta_k = 0$  for the non-minimal  $\Delta_k$ , where  $k \in \{1, 2, 3\}$ , while ensuring that the sum of the remaining  $\beta_k$ , which are associated with minimal  $\Delta_k$  equals 1. Thus, the optimum should satisfy:

$$\begin{aligned} & \beta_k = 0, \quad \forall \Delta_k \neq \Delta_{\min} \\ & \sum_{k: \Delta_k = \Delta_{\min}} \beta_k = 1, \end{aligned} \quad (15)$$

where  $\Delta_{\min} = \min\{\Delta_1, \Delta_2, \Delta_3\}$ .

## IV. STRATEGY OPTIMIZATION

### A. Initial Resource Allocation Optimization

We first maximize the distortion of *Eve* based on a deterministic decryptor.

$$(OP) : \underset{n_M, n_K}{\text{maximize}} \quad D_{\text{Eve}} \quad (16a)$$

$$\text{subject to} \quad n_M, n_K \in \mathbb{Z}^+, \quad (16b)$$

$$\varepsilon_{\text{Bob},M} \leq \varepsilon_{\text{Bob},M}^{\text{th}}, \quad (16c)$$

$$\varepsilon_{\text{Eve},M} \leq \varepsilon_{\text{Eve},M}^{\text{th}}, \quad (16d)$$

$$\varepsilon_{\text{Bob},K} \leq \varepsilon_{\text{Bob},K}^{\text{th}}, \quad (16e)$$

$$\varepsilon_{\text{Eve},K} \geq \varepsilon_{\text{Eve},K}^{\text{th}}, \quad (16f)$$

$$D_{\text{Bob}} \leq D_{\text{Bob}}^{\text{th}} \quad (16g)$$

where  $D_{\text{Eve}} = \varepsilon_{\text{Eve},M} D_{\text{loss}} + \alpha(1 - \varepsilon_{\text{Eve},M}) \varepsilon_{\text{Eve},K} D_{\text{conf}}$ .

Without loss of generality, we assume the data is transmitted over additive white Gaussian noise (AWGN) channel in this paper. It is worth noting that in the case of more complex channels, such as fading channels, dynamic CSI will certainly lead to a suboptimal configuration of the PLD scheme, which may result in performance degradation. To overcome this limitation, artificial intelligence (AI)-based channel prediction techniques offer a promising solution.

According to [28], the error probability  $\varepsilon_{i,j}$  with a given packet size  $d_j$  can be written as  $\varepsilon_{i,j} = Q\left(\sqrt{\frac{n_j}{V(\gamma_i)}}(\mathcal{C}(\gamma_i) - \frac{d_j}{n_j})\ln 2\right)$ , where  $Q(x) = \frac{1}{\sqrt{2\pi}} \int_x^\infty e^{-t^2/2} dt$  is the Q-function in statistic,  $\mathcal{C}(\gamma_i) = \log_2(1 + \gamma_i)$  is the Shannon capacity,  $V(\gamma_i) = 1 - \frac{1}{(1+\gamma_i)^2}$  is the channel dispersion with  $\lambda_i = \frac{z_i P}{\sigma^2}$ .

**Theorem 1.** *The maximum of  $D_{\text{Eve}}$  is achieved at  $(n_{\text{M}}^{\max}, n_{\text{K}}^{\min})$  when  $\alpha \geq \frac{D_{\text{loss}}}{\varepsilon_{\text{Eve},\text{K}}^{\max} D_{\text{conf}}}$ , while achieved at  $(n_{\text{M}}^{\min}, n_{\text{K}}^{\min})$  when  $\alpha < \frac{D_{\text{loss}}}{\varepsilon_{\text{Eve},\text{K}}^{\max} D_{\text{conf}}}$ .*

This theorem indicates that the optimal resource allocation scheme is always achieved at the boundary. The coding rate of the key should always be maximized to prevent *Eve* from decoding it, whereas the optimal coding rate of the ciphertext is determined by the ciphering probability  $\alpha$ . When the  $\alpha$  is high, more valid keys are transmitted, making the distortion caused by confusion more significant than that resulting from message loss. Consequently, the optimal coding rate of the ciphertext should be minimized to ensure correct decoding. Conversely, when the ciphering probability is low, litter sequences are transmitted more frequently, so the distortion due to information loss becomes dominant. In this case, the coding rate of the ciphertext should be maximized to maximize the distortion associated with message loss.

*Proof.* We first investigate the monotonicity of  $\varepsilon_{i,j}$  with respect to  $n_j$ . In particular, we have

$$\frac{\partial \varepsilon_{i,j}}{\partial n_j} = \frac{\partial \varepsilon_{i,j}}{\partial w_{i,j}} \frac{\partial w_{i,j}}{\partial n_j} < 0, \quad (17)$$

where

$$\frac{\partial \varepsilon_{i,j}}{\partial w_{i,j}} = \frac{\partial \left( \int_{w_{i,j}}^\infty \frac{1}{\sqrt{2\pi}} e^{-t^2/2} dt \right)}{\partial w_{i,j}} = -\frac{1}{\sqrt{2\pi}} e^{-\frac{w_{i,j}^2}{2}} < 0, \quad (18)$$

$$\frac{\partial w_{i,j}}{\partial n_j} = \frac{1}{2} n_j^{-\frac{1}{2}} V_{i,j}^{-\frac{1}{2}} \mathcal{C}_{i,j} \ln 2 + \frac{1}{2} n_j^{-\frac{3}{2}} V_{i,j}^{-\frac{1}{2}} d_j \ln 2 > 0. \quad (19)$$

Thus,  $\varepsilon_{i,j}$  is monotonically decreasing in  $n_j$ . We can easily derive the monotonicity of  $D_{\text{Eve}}$  for  $n_{\text{M}}$  and  $n_{\text{K}}$  respectively:

$$\frac{\partial D_{\text{Eve}}}{\partial n_{\text{M}}} = \frac{\partial \varepsilon_{\text{Eve},\text{M}}}{\partial n_{\text{M}}} (D_{\text{loss}} - \alpha \varepsilon_{\text{Eve},\text{K}} D_{\text{conf}}) \quad (20)$$

$$\frac{\partial D_{\text{Eve}}}{\partial n_{\text{K}}} = \frac{\partial \varepsilon_{\text{Eve},\text{K}}}{\partial n_{\text{K}}} \alpha (1 - \varepsilon_{\text{Eve},\text{M}}) D_{\text{conf}} < 0 \quad (21)$$

From (21) we know that  $D_{\text{Eve}}$  is monotonically decreasing in  $n_{\text{K}}$ , while the monotonicity of  $D_{\text{Eve}}$  in  $n_{\text{M}}$  depends on  $(D_{\text{loss}} - \alpha \varepsilon_{\text{Eve},\text{K}} D_{\text{conf}})$  according to (20). Thus, the optimal  $(n_{\text{M}}, n_{\text{K}})$  must be located at the boundary.

Since the monotonically decreasing property of  $D_{\text{Eve}}$  with respect to  $n_{\text{K}}$  is deterministic, the maximum of  $D_{\text{Eve}}$  must be obtained at the  $n_{\text{K}}^{\min}$ . Thus, we can first derive the expression of  $n_{\text{K}}^{\min}$ . The feasible range of  $n_{\text{K}}$  is limited by constraints (16e)-(16g). To obtain the lower bound of  $n_{\text{K}}$ , we first investigate the upper bound  $\varepsilon_{\text{Bob},\text{K}}$  according to the monotonicity of  $\varepsilon_{i,\text{K}}$  with respect to  $n_{\text{K}}$ . From constraint (16g) we have:

$$\varepsilon_{\text{Bob},\text{K}} \leq \frac{D_{\text{Bob}}^{\text{th}} - \varepsilon_{\text{Bob},\text{M}} D_{\text{loss}}}{\alpha(1 - \varepsilon_{\text{Bob},\text{M}}) D_{\text{conf}}}. \quad (22)$$

We define  $f(\varepsilon_{\text{Bob},\text{M}}) = \frac{D_{\text{Bob}}^{\text{th}} - \varepsilon_{\text{Bob},\text{M}} D_{\text{loss}}}{\alpha(1 - \varepsilon_{\text{Bob},\text{M}}) D_{\text{conf}}}$ . To obtain the maximum of  $f(\varepsilon_{\text{Bob},\text{M}})$ , we first calculate the first-order derivative  $f'(\varepsilon_{\text{Bob},\text{M}})$ :

$$\frac{\partial f(\varepsilon_{\text{Bob},\text{M}})}{\partial \varepsilon_{\text{Bob},\text{M}}} = \frac{D_{\text{conf}}(D_{\text{Bob}}^{\text{th}} - D_{\text{loss}})}{\alpha[(1 - \varepsilon_{\text{Bob},\text{M}}) D_{\text{conf}}]^2}. \quad (23)$$

Since we need to set the  $D_{\text{Bob}}^{\text{th}}$  as small as possible to limit *Bob*'s distortion, the inequality  $D_{\text{Bob}}^{\text{th}} < D_{\text{loss}}$  always holds. Thus,  $\frac{\partial f(\varepsilon_{\text{Bob},\text{M}})}{\partial \varepsilon_{\text{Bob},\text{M}}} < 0$ , which means  $f(\varepsilon_{\text{Bob},\text{M}})$  is monotonically decreasing for  $\varepsilon_{\text{Bob},\text{M}} > 0$ . For  $\varepsilon_{\text{Bob},\text{M}} > 0$  we have  $\varepsilon_{\text{Bob},\text{K}} < f(\varepsilon_{\text{Bob},\text{M}} = 0)$ . Therefore, we derive another upper bound of  $\varepsilon_{\text{Bob},\text{K}}$ :

$$\varepsilon_{\text{Bob},\text{K}} < \frac{D_{\text{Bob}}^{\text{th}}}{\alpha D_{\text{conf}}}. \quad (24)$$

Combining (16e), we can obtain the upper bound of  $\varepsilon_{\text{Bob},\text{K}}$  by comparing the two constraints:

$$\varepsilon_{\text{Bob},\text{K}}^{\max} = \min \left\{ \varepsilon_{\text{Bob},\text{K}}^{\text{th}}, \frac{D_{\text{Bob}}^{\text{th}}}{\alpha D_{\text{conf}}} \right\}. \quad (25)$$

We can derive the expression of blocklength  $n$  with respect to error probability  $\varepsilon$  based on Polyanskiy's paper [28]. To simplify the subsequent analysis, we introduce an auxiliary function  $\phi(\varepsilon_{i,j})$  to represent the blocklength  $n_j$  required to achieve a specific error probability  $\varepsilon_{i,j}$ , given the payload  $d_j$  and signal-to-noise ratio (SNR)  $\gamma_i$ . This function can be expressed as follows:

$$\phi(\varepsilon_{i,j}) = \left( \frac{\log_2 e \mathcal{Q}^{-1}(\varepsilon_{i,j}) \sqrt{V_i}}{2 \mathcal{C}_i} + \frac{\sqrt{[(\log_2 e \mathcal{Q}^{-1}(\varepsilon_{i,j})]^2 V_i + 4 d_j \mathcal{C}_i}}{2 \mathcal{C}_i} \right)^2. \quad (26)$$

Thus, the  $n_{\text{K}}^{\min}$  can be presented as:

$$n_{\text{K}}^{\min} = \phi(\varepsilon_{\text{Bob},\text{K}}^{\max}). \quad (27)$$

Next, we derive the range of values of  $n_{\text{M}}$  in the same way. The feasible range of  $n_{\text{M}}$  is determined by constraints (16c)-(16d) and (16g). Since both  $\varepsilon_{\text{Bob},\text{M}}$  and  $\varepsilon_{\text{Eve},\text{M}}$  are monotonically decreasing in  $n_{\text{M}}$ , these two constraints can only limit the lower bound of  $n_{\text{M}}$ . From constraint (16g) we can derive that  $\varepsilon_{\text{Bob},\text{M}}(D_{\text{loss}} - \varepsilon_{\text{Bob},\text{K}} \alpha D_{\text{conf}}) \leq \tilde{D}_{\text{Bob}}^{\text{th}} - \varepsilon_{\text{Bob},\text{K}} \alpha D_{\text{conf}}$ . From the upper bound of  $\varepsilon_{\text{Bob},\text{K}}$  in (22) we can derive that  $D_{\text{loss}} - \varepsilon_{\text{Bob},\text{K}} \alpha D_{\text{conf}} > \frac{D_{\text{loss}} - D_{\text{Bob}}^{\text{th}}}{1 - \varepsilon_{\text{Bob},\text{M}}}$ . Since we assume that  $D_{\text{loss}} > D_{\text{Bob}}^{\text{th}}$  always holds, we can know that

$D_{\text{loss}} - \varepsilon_{\text{Bob},\text{K}} \alpha D_{\text{conf}} > 0$ . Thus, the upper bound of  $\varepsilon_{\text{Bob},\text{M}}$  can be :

$$\varepsilon_{\text{Bob},\text{M}} \leq \frac{\tilde{D}_{\text{Bob}}^{\text{th}} - \varepsilon_{\text{Bob},\text{K}} \alpha D_{\text{conf}}}{D_{\text{loss}} - \varepsilon_{\text{Bob},\text{K}} \alpha D_{\text{conf}}}. \quad (28)$$

To simplify (28), we define  $g(\varepsilon_{\text{Bob},\text{K}}) = \frac{D_{\text{Bob}}^{\text{th}} - \alpha \varepsilon_{\text{Bob},\text{K}} D_{\text{conf}}}{D_{\text{loss}} - \alpha \varepsilon_{\text{Bob},\text{K}} D_{\text{conf}}}$  and investigate the monotonicity of  $g(\varepsilon_{\text{Bob},\text{K}})$ :

$$\frac{\partial g(\varepsilon_{\text{Bob},\text{K}})}{\partial \varepsilon_{\text{Bob},\text{K}}} = \frac{\alpha D_{\text{conf}} (D_{\text{Bob}}^{\text{th}} - D_{\text{loss}})}{(D_{\text{loss}} - \alpha \varepsilon_{\text{Bob},\text{K}} D_{\text{conf}})^2}. \quad (29)$$

We always set  $D_{\text{Bob}}^{\text{th}}$  as small as possible to ensure that  $D_{\text{Bob}}^{\text{th}} < D_{\text{loss}}$ . Thus,  $\frac{\partial g(\varepsilon_{\text{Bob},\text{K}})}{\partial \varepsilon_{\text{Bob},\text{K}}} < 0$ , which means that  $g(\varepsilon_{\text{Bob},\text{K}})$  is monotonically decreasing with respect to  $\varepsilon_{\text{Bob},\text{K}}$ . From  $\varepsilon_{\text{Bob},\text{K}} > 0$  we can derive that  $g(\varepsilon_{\text{Bob},\text{K}}) < \frac{D_{\text{Bob}}^{\text{th}}}{D_{\text{loss}}}$ . Thus, the upper bound (28) can be simplified to:

$$\varepsilon_{\text{Bob},\text{M}} \leq \frac{D_{\text{Bob}}^{\text{th}}}{D_{\text{loss}}}. \quad (30)$$

Thus, the constraints (16c)-(16d) and (16g) only determine the  $n_{\text{M}}^{\text{min}}$ . Next, according to constraints (16c) and (16d), we can find the maximum of  $\varepsilon_{\text{Bob},\text{M}}$ :

$$\varepsilon_{\text{Bob},\text{M}}^{\text{max}} = \min \left\{ \varepsilon_{\text{Bob},\text{M}}^{\text{th}}, \frac{D_{\text{Bob}}^{\text{th}}}{D_{\text{loss}}} \right\} \quad (31)$$

From  $\varepsilon_{\text{Bob},\text{M}} \leq \varepsilon_{\text{Bob},\text{M}}^{\text{max}}$  and the monotonically decreasing property of  $\varepsilon_{i,j}$  for  $n_j$ , we can derive that  $n_{\text{M}} \geq \phi(\varepsilon_{\text{Bob},\text{M}}^{\text{max}})$ . Besides, from constraint (16d) we know that  $n_{\text{M}} \geq \phi(\varepsilon_{\text{Eve},\text{M}}^{\text{th}})$ . Thus, the minimum of  $n_{\text{M}}$  can be expressed as:

$$n_{\text{M}}^{\text{min}} = \min \{ \phi(\varepsilon_{\text{Bob},\text{M}}^{\text{max}}), \phi(\varepsilon_{\text{Eve},\text{M}}^{\text{th}}) \}. \quad (32)$$

From (27), the value of  $n_{\text{K}}$  is determined. Substituting this value into (20) allows us to characterize the monotonic behavior of  $D_{\text{Eve}}$  with respect to  $n_{\text{M}}$ . From  $n_{\text{K}}^{\text{min}}$  we can calculate the  $\varepsilon_{\text{Eve},\text{K}}^{\text{max}}$ , so in this case the monotonicity of  $D_{\text{Eve}}$  only depends on the value of  $\alpha$ . If  $\alpha \geq \frac{D_{\text{loss}}}{\varepsilon_{\text{Eve},\text{K}}^{\text{max}} D_{\text{conf}}}$ ,  $D_{\text{Eve}}$  is monotonically increasing with respect to  $n_{\text{M}}$ . The maximum of  $D_{\text{Eve}}$  is obtained at  $(n_{\text{M}}^{\text{max}}, n_{\text{K}}^{\text{min}})$ , whose analytic solutions are calculated in (27) and (32). We only need to take the largest possible value for  $n_{\text{M}}$  according to the requirements in practical application.

When  $\alpha < \frac{D_{\text{loss}}}{\varepsilon_{\text{Eve},\text{K}}^{\text{max}} D_{\text{conf}}}$ ,  $D_{\text{Eve}}$  is monotonically decreasing with respect to  $n_{\text{M}}$ . Thus, the maximum of  $D_{\text{Eve}}$  is achieved at  $(n_{\text{M}}^{\text{min}}, n_{\text{K}}^{\text{min}})$ , whose analytic solution is expressed in (32) and (27).

In summary, the maximum of  $D_{\text{Eve}}$  can be formulated as:

$$D_{\text{Eve}}^{\text{max}} = \begin{cases} \varepsilon_{\text{Eve},\text{M}}^{\text{max}} + \\ \alpha [1 - \varepsilon_{\text{Eve},\text{M}}^{\text{max}}] \varepsilon_{\text{Eve},\text{K}}^{\text{max}} D_{\text{conf}} & \text{if } \alpha < \frac{D_{\text{loss}}}{\varepsilon_{\text{Eve},\text{K}}^{\text{max}} D_{\text{conf}}} \\ \varepsilon_{\text{Eve},\text{M}}^{\text{min}} + \\ \alpha [1 - \varepsilon_{\text{Eve},\text{M}}^{\text{min}}] \varepsilon_{\text{Eve},\text{K}}^{\text{max}} D_{\text{conf}} & \text{if } \alpha \geq \frac{D_{\text{loss}}}{\varepsilon_{\text{Eve},\text{K}}^{\text{max}} D_{\text{conf}}} \end{cases} \quad (33)$$

where:

$$\varepsilon_{\text{Eve},\text{K}}^{\text{max}} = \mathcal{Q} \left( \ln 2 \sqrt{\frac{\phi \left( \min \left\{ \varepsilon_{\text{Bob},\text{K}}^{\text{th}}, \frac{D_{\text{Bob}}^{\text{th}}}{\alpha D_{\text{conf}}} \right\} \right)}{V_{\text{Eve}}}} \right. \\ \left. \cdot \left( \mathcal{C}_{\text{Eve}} - \frac{d_{\text{K}}}{\phi \left( \min \left\{ \varepsilon_{\text{Bob},\text{K}}^{\text{th}}, \frac{D_{\text{Bob}}^{\text{th}}}{\alpha D_{\text{conf}}} \right\} \right)} \right) \right), \quad (34)$$

$$\varepsilon_{\text{Eve},\text{M}}^{\text{max}} = \mathcal{Q} \left( \ln 2 \sqrt{\frac{\min \left\{ \phi \left( \frac{D_{\text{Bob}}^{\text{th}}}{D_{\text{loss}}} \right), \phi \left( \varepsilon_{\text{Eve},\text{M}}^{\text{th}} \right) \right)}{V_{\text{Eve}}}} \right. \\ \left. \cdot \left( \mathcal{C}_{\text{Eve}} - \frac{d_{\text{M}}}{\min \left\{ \phi \left( \frac{D_{\text{Bob}}^{\text{th}}}{D_{\text{loss}}} \right), \phi \left( \varepsilon_{\text{Eve},\text{M}}^{\text{th}} \right) \right)} \right) \right), \quad (35)$$

$$\varepsilon_{\text{Eve},\text{M}}^{\text{min}} = \mathcal{Q} \left( \ln 2 \sqrt{\frac{n_{\text{M}}^{\text{max}}}{V_{\text{Eve}}}} \left( \mathcal{C}_{\text{Eve}} - \frac{d_{\text{M}}}{n_{\text{M}}^{\text{max}}} \right) \right). \quad (36)$$

□

## B. Ciphering Probability Optimization

We assume that *Alice* has a full knowledge of the decryption strategy of *Bob* and *Eve*. In this case, *Alice* can calculate the  $(\varepsilon_{\text{Bob},\text{M}}, \varepsilon_{\text{Bob},\text{K}})$  based on fixed radio resource allocation and accurate CSI. Therefore, *Bob*'s optimal decryption strategy and the corresponding  $\min(\tilde{D}_{\text{Bob}})$ , which is the function of the ciphering probability  $\alpha$ , can be predicted by *Alice*.

On the other hand, *Alice* can estimate *Eve*'s expected error probabilities based on the statistical knowledge of the eavesdropping channel condition. Thus, *Alice* can also predict *Eve*'s optimal strategy, which is denoted as  $\min(\tilde{D}_{\text{Eve}}(\mathbb{E}\{\varepsilon_{\text{Eve},\text{M}}\}, \mathbb{E}\{\varepsilon_{\text{Eve},\text{K}}\}))$ .

By adjusting the deceptive encryptor's activation rate  $\alpha$ , *Alice* is able to optimize the semantic secrecy performance. The optimization problem can be presented as:

$$\underset{\alpha}{\text{maximize}} \quad \min \tilde{D}_{\text{Eve}}(\mathbb{E}\{\varepsilon_{\text{Eve},\text{M}}\}, \mathbb{E}\{\varepsilon_{\text{Eve},\text{K}}\}) \quad (37a)$$

$$\text{subject to} \quad \min \tilde{D}_{\text{Bob}} \leq \tilde{D}_{\text{Bob}}^{\text{th}}, \quad (37b)$$

where  $\tilde{D}_{\text{Bob}}^{\text{th}}$  is the predefined threshold. Since the objective function and constraint in Problem (37) are both linear, this problem is convex. Therefore, the optimal  $\alpha$  is always obtained at the boundary, and we can directly calculate the expression of the optimal  $\alpha^o$  for different decryption strategies of Eve and Bob. When  $\beta_1^{\text{Eve}} = 1$ ,  $\min \tilde{D}_{\text{Eve}}$  is monotonically increasing with respect to  $\alpha$ . Thus, the optimal  $\alpha^o$  is obtained at the maximum:

$$\alpha^o = \begin{cases} \min \left\{ \frac{\tilde{D}_{\text{Bob}}^{\text{th}} - \varepsilon_{\text{Bob},\text{M}} D_{\text{loss}}}{(1 - \varepsilon_{\text{Bob},\text{M}}) \varepsilon_{\text{Bob},\text{K}} D_{\text{conf}}}, 1 \right\} & \text{if } \beta_1^{\text{Bob}} = 1 \\ 1 & \text{if } \beta_2^{\text{Bob}} = 1 \\ 1 & \text{if } \beta_3^{\text{Bob}} = 1. \end{cases} \quad (38)$$

When  $\beta_2^{\text{Eve}} = 1$  or  $\beta_3^{\text{Eve}} = 1$ ,  $\min \tilde{D}_{\text{Eve}}$  is monotonically decreasing with respect to  $\alpha$ . The optimal  $\alpha^o$  is obtained at

the minimum:

$$\alpha^o = \begin{cases} 0 & \text{if } \beta_1^{\text{Bob}} = 1 \\ \frac{D_{\text{loss}} - \tilde{D}_{\text{Bob}}^{\text{th}}}{(1 - \varepsilon_{\text{Bob},K})(1 - \varepsilon_{\text{Bob},M})D_{\text{loss}}} & \text{if } \beta_2^{\text{Bob}} = 1 \\ \max \left\{ \frac{(S-1)}{[(S-2)\varepsilon_{\text{Bob},K} - (S-1)]}, \frac{[\tilde{D}_{\text{Bob}}^{\text{th}} - \varepsilon_{\text{Bob},M}D_{\text{loss}} - (1 - \varepsilon_{\text{Bob},M})D_{\text{conf}}]}{(1 - \varepsilon_{\text{Bob},M})D_{\text{conf}}}, 0 \right\} & \text{if } \beta_3^{\text{Bob}} = 1. \end{cases} \quad (39)$$

### C. Adaptive Resource Allocation Optimization

Based on the optimized  $\alpha^o$ , we can further maximize  $\min \tilde{D}_{\text{Eve}}(\mathbb{E}\{\varepsilon_{\text{Eve},M}\}, \mathbb{E}\{\varepsilon_{\text{Eve},K}\}, \alpha^o)$  by optimizing the resource allocation scheme. Thus, the new optimization problem can be presented as:

$$\text{maximize}_{n_M, n_K} \quad \min \tilde{D}_{\text{Eve}}(\mathbb{E}\{\varepsilon_{\text{Eve},M}\}, \mathbb{E}\{\varepsilon_{\text{Eve},K}\}, \alpha^o) \quad (40a)$$

$$\text{subject to} \quad (16b) - (16f), \quad (40b)$$

$$\min \tilde{D}_{\text{Bob}}(\alpha^o) \leq \tilde{D}_{\text{Bob}}^{\text{th}}. \quad (40c)$$

To solve this problem, we need to consider three decryption strategies for *Eve* separately. Besides, the maximum  $\min \tilde{D}_{\text{Eve}}$  is also affected by the boundary points according to constraint (40c). In other words, it depends on *Alice*'s prediction of the decryption strategy that *Bob* will adopt. For ease of discussion, we first simplify the constraints and determine the ranges of  $n_M$  and  $n_K$  under the three decryption strategies for *Bob*.

#### 1) Boundary for *Bob*'s Perception Strategy

If *Alice* predicts that *Bob* will select the strategy *Perception*, i.e.,  $\beta_1^{\text{Bob}} = 1$ , the expression of  $\min \tilde{D}_{\text{Bob}}$  is  $\tilde{D}_{\text{Bob}}^{\beta_1} = \varepsilon_{\text{Bob},M}D_{\text{loss}} + \alpha^o(1 - \varepsilon_{\text{Bob},M})\varepsilon_{\text{Bob},M}D_{\text{conf}}$ . This expression is the same as the constraint (16g). Thus, we can simplify the constraints as follows:

$$\varepsilon_{\text{Bob},K} \leq \frac{\tilde{D}_{\text{Bob}}^{\text{th}}}{\alpha^o D_{\text{conf}}}, \quad (41)$$

$$\varepsilon_{\text{Bob},M} \leq \frac{\tilde{D}_{\text{Bob}}^{\text{th}}}{D_{\text{loss}}}. \quad (42)$$

The minimum of  $n_M$  and  $n_K$  can be formulated as:

$$n_M^{\min} = \min \left\{ \phi(\varepsilon_{\text{Eve},M}^{\text{th}}), \phi\left(\frac{\tilde{D}_{\text{Bob}}^{\text{th}}}{D_{\text{loss}}}\right) \right\} \quad (43)$$

$$n_K^{\min} = \phi \left[ \min \left( \varepsilon_{\text{Bob},K}^{\text{th}}, \frac{\tilde{D}_{\text{Bob}}^{\text{th}}}{\alpha^o D_{\text{conf}}} \right) \right]. \quad (44)$$

#### 2) Boundary for *Bob*'s Dropping Strategy

If *Alice* predicts that *Bob* will select the strategy *Dropping*, i.e.  $\beta_2^{\text{Bob}} = 1$ , then  $\tilde{D}_{\text{Bob}}^{\beta_2} = \varepsilon_{\text{Bob},M}D_{\text{loss}} + (1 - \varepsilon_{\text{Bob},M})[\varepsilon_{\text{Bob},K}\alpha^o + (1 - \alpha^o)]D_{\text{loss}}$ . The upper bound of  $\varepsilon_{\text{Bob},K}$  derived from constraint (40c) is:

$$\varepsilon_{\text{Bob},K} \leq \frac{\tilde{D}_{\text{Bob}}^{\text{th}} - \varepsilon_{\text{Bob},M}D_{\text{loss}}}{\alpha^o(1 - \varepsilon_{\text{Bob},M})D_{\text{loss}}} + \frac{\alpha^o - 1}{\alpha^o}. \quad (45)$$

To simplify this expression, we define  $h(\varepsilon_{\text{Bob},M}) = \frac{\tilde{D}_{\text{Bob}}^{\text{th}} - \varepsilon_{\text{Bob},M}D_{\text{loss}}}{\alpha^o(1 - \varepsilon_{\text{Bob},M})D_{\text{loss}}} + \frac{\alpha^o - 1}{\alpha^o}$  and calculate the first-order derivative:

$$\frac{\partial h(\varepsilon_{\text{Bob},M})}{\partial \varepsilon_{\text{Bob},M}} = \frac{\alpha^o D_{\text{loss}}(\tilde{D}_{\text{Bob}}^{\text{th}} - D_{\text{loss}})}{[\alpha^o(1 - \varepsilon_{\text{Bob},M})D_{\text{loss}}]^2} < 0, \quad (46)$$

which indicates that  $h(\varepsilon_{\text{Bob},M})$  is monotonically decreasing. Thus, from  $\varepsilon_{\text{Bob},M} > 0$  we can derive that  $\varepsilon_{\text{Bob},K} < h(\varepsilon_{\text{Bob},M} = 0)$ . This upper bound can be presented as:

$$\varepsilon_{\text{Bob},K} \leq \frac{\tilde{D}_{\text{Bob}}^{\text{th}} + (\alpha^o - 1)D_{\text{loss}}}{\alpha^o D_{\text{loss}}}. \quad (47)$$

In the same way, we can obtain the upper bound of  $\varepsilon_{\text{Bob},M}$ :

$$\varepsilon_{\text{Bob},M} \leq 1 - \frac{D_{\text{loss}} - \tilde{D}_{\text{Bob}}^{\text{th}}}{\alpha^o D_{\text{loss}}(1 - \varepsilon_{\text{Bob},K})}. \quad (48)$$

Since we usually set the  $\tilde{D}_{\text{Bob}}^{\text{th}}$  small enough so that inequality  $\tilde{D}_{\text{Bob}}^{\text{th}} < D_{\text{loss}}$  always holds. Thus, from  $\varepsilon_{\text{Bob},K} > 0$  we can obtain the upper bound:

$$\varepsilon_{\text{Bob},M} \leq 1 - \frac{D_{\text{loss}} - \tilde{D}_{\text{Bob}}^{\text{th}}}{\alpha^o D_{\text{loss}}}. \quad (49)$$

Thus, the lower bound of  $n_M$  and  $n_K$  can be expressed as:

$$n_M^{\min} = \min \left\{ \phi(\varepsilon_{\text{Eve},M}^{\text{th}}), \phi\left(1 - \frac{D_{\text{loss}} - \tilde{D}_{\text{Bob}}^{\text{th}}}{\alpha^o D_{\text{loss}}}\right) \right\} \quad (50)$$

$$n_K^{\min} = \phi \left[ \min \left( \varepsilon_{\text{Bob},K}^{\text{th}}, \frac{\tilde{D}_{\text{Bob}}^{\text{th}} + (\alpha^o - 1)D_{\text{loss}}}{\alpha^o D_{\text{loss}}} \right) \right]. \quad (51)$$

#### 3) Boundary for *Bob*'s Exclusion Strategy

Finally, if *Alice* predicts that *Bob* will select the strategy *Exclusion*, i.e.,  $\beta_3^{\text{Bob}} = 1$ , then  $\tilde{D}_{\text{Bob}}^{\beta_3} = \varepsilon_{\text{Bob},M}D_{\text{loss}} + (1 - \varepsilon_{\text{Bob},M})[\varepsilon_{\text{Bob},K}\alpha^o + (1 - \alpha^o)]D_{\text{loss}}$ . We can derive the upper bound of  $\varepsilon_{\text{Bob},K}$  as follows:

$$\varepsilon_{\text{Bob},K} \leq \frac{\tilde{D}_{\text{Bob}}^{\text{th}} - \varepsilon_{\text{Bob},M}D_{\text{loss}}(S-1)}{\alpha^o(S-2)D_{\text{conf}}(1 - \varepsilon_{\text{Bob},M})} - \frac{(1 - \alpha^o)(S-1)(1 - \varepsilon_{\text{Bob},M})D_{\text{conf}}}{\alpha^o(S-2)D_{\text{conf}}(1 - \varepsilon_{\text{Bob},M})}. \quad (52)$$

We define the function  $j(\varepsilon_{\text{Bob},M}) = \frac{\tilde{D}_{\text{Bob}}^{\text{th}} - \varepsilon_{\text{Bob},M}D_{\text{loss}}(S-1)}{\alpha^o(S-2)D_{\text{conf}}(1 - \varepsilon_{\text{Bob},M})} - \frac{(1 - \alpha^o)(S-1)(1 - \varepsilon_{\text{Bob},M})D_{\text{conf}}}{\alpha^o(S-2)D_{\text{conf}}(1 - \varepsilon_{\text{Bob},M})}$  and then calculate the first-order derivative:

$$\frac{\partial j(\varepsilon_{\text{Bob},M})}{\partial \varepsilon_{\text{Bob},M}} = \frac{[\tilde{D}_{\text{Bob}}^{\text{th}} - D_{\text{loss}}(S-1)]}{\alpha^o(S-2)D_{\text{conf}}} - \frac{\alpha^o(S-2)D_{\text{conf}}}{[\alpha^o(S-2)D_{\text{conf}}(1 - \varepsilon_{\text{Bob},M})]^2}. \quad (53)$$

Since we always set  $\tilde{D}_{\text{Bob}}^{\text{th}}$  as small as possible, the inequality  $\tilde{D}_{\text{Bob}}^{\text{th}} < D_{\text{loss}}(S-1)$  always holds. Thus,  $\frac{\partial j(\varepsilon_{\text{Bob},M})}{\partial \varepsilon_{\text{Bob},M}} < 0$ , which means that  $j(\varepsilon_{\text{Bob},M})$  is monotonically decreasing with respect to  $\varepsilon_{\text{Bob},M}$ . From  $\varepsilon_{\text{Bob},M} > 0$  we can derive that  $\varepsilon_{\text{Bob},K} < j(\varepsilon_{\text{Bob},M} = 0)$ . Thus, the upper bound of  $\varepsilon_{\text{Bob},K}$  can be simplified as:

$$\varepsilon_{\text{Bob},K} \leq \frac{\tilde{D}_{\text{Bob}}^{\text{th}} - (1 - \alpha^o)(S-1)D_{\text{conf}}}{\alpha^o(S-2)D_{\text{conf}}}. \quad (54)$$

Next, we drive the upper bound of  $\varepsilon_{\text{Bob},M}$  with  $\beta_3^{\text{Bob}} = 1$ :

$$\varepsilon_{\text{Bob},M} \leq \frac{\tilde{D}_{\text{Bob}}^{\text{th}} - (1 - \alpha^o)D_{\text{conf}} - \varepsilon_{\text{Bob},K} \frac{\alpha^o(S-2)}{S-1} D_{\text{conf}}}{D_{\text{loss}} - (1 - \alpha^o)D_{\text{conf}} - \varepsilon_{\text{Bob},K} \frac{\alpha^o(S-2)}{S-1} D_{\text{conf}}}. \quad (55)$$

We then define the function  $k(\varepsilon_{\text{Bob},K}) = \frac{\tilde{D}_{\text{Bob}}^{\text{th}} - (1 - \alpha^0)D_{\text{conf}} - \varepsilon_{\text{Bob},K} \frac{\alpha^0(\mathcal{S}-2)}{\mathcal{S}-1} D_{\text{conf}}}{D_{\text{loss}} - (1 - \alpha^0)D_{\text{conf}} - \varepsilon_{\text{Bob},K} \frac{\alpha^0(\mathcal{S}-2)}{\mathcal{S}-1} D_{\text{conf}}}$  and calculate the first-order derivative:

$$\frac{\partial k(\varepsilon_{\text{Bob},K})}{\partial \varepsilon_{\text{Bob},K}} = \frac{\alpha^0(\mathcal{S}-2)}{\mathcal{S}-1} \frac{(\tilde{D}_{\text{Bob}}^{\text{th}} - D_{\text{loss}})D_{\text{conf}}}{\left[ D_{\text{loss}} - (1 - \alpha^0)D_{\text{conf}} - \varepsilon_{\text{Bob},K} \frac{\alpha^0(\mathcal{S}-2)}{\mathcal{S}-1} D_{\text{conf}} \right]^2} \quad (56)$$

Since the cardinality of the codebook  $\mathcal{S} \geq 2$  and we always assume that  $\tilde{D}_{\text{Bob}}^{\text{th}} < D_{\text{loss}}$ , we can obtain  $\frac{\partial k(\varepsilon_{\text{Bob},K})}{\partial \varepsilon_{\text{Bob},K}} < 0$ , which means that  $k(\varepsilon_{\text{Bob},K})$  is decreasing monotonically with respect to  $\varepsilon_{\text{Bob},K}$ . From  $\varepsilon_{\text{Bob},K} > 0$  we can derive that  $\varepsilon_{\text{Bob},M} < k(\varepsilon_{\text{Bob},K} = 0)$ . Thus, the upper bound of  $\varepsilon_{\text{Bob},M}$  can be simplified as follows:

$$\varepsilon_{\text{Bob},M} \leq \frac{\tilde{D}_{\text{Bob}}^{\text{th}} - (1 - \alpha^0)D_{\text{conf}}}{D_{\text{loss}} - (1 - \alpha^0)D_{\text{conf}}}. \quad (57)$$

Thus, the minimum of  $n_M$  and  $n_K$  can be formulated as:

$$n_M^{\min} = \min \left\{ \phi \left( \varepsilon_{\text{Eve},M}^{\text{th}} \right), \phi \left( \frac{\tilde{D}_{\text{Bob}}^{\text{th}} - (1 - \alpha^0)D_{\text{conf}}}{D_{\text{loss}} - (1 - \alpha^0)D_{\text{conf}}} \right) \right\} \quad (58)$$

$$n_K^{\min} = \phi \left[ \min \left( \varepsilon_{\text{Bob},K}^{\text{th}}, \frac{\tilde{D}_{\text{Bob}}^{\text{th}} - (1 - \alpha^0)(\mathcal{S}-1)D_{\text{conf}}}{\alpha^0(\mathcal{S}-2)D_{\text{conf}}} \right) \right] \quad (59)$$

It is worth noting that, since the maximum value of  $D_{\text{Eve}}$  always occurs at the minimum value of  $n_K$ , we do not consider the maximum value of  $n_K$ . Moreover, as there is no constraint on the maximum value of  $n_M$  in the given conditions,  $n_M^{\max}$  is determined according to practical requirements. Therefore, we summarize the minimum values of  $n_K$  and  $n_M$  under different decryption strategies adopted by *Bob*:

$$n_M^{\min} = \begin{cases} \min \left\{ \phi \left( \varepsilon_{\text{Eve},M}^{\text{th}} \right), \phi \left( \frac{\tilde{D}_{\text{Bob}}^{\text{th}}}{D_{\text{loss}}} \right) \right\} & \text{if } \beta_1^{\text{Bob}} = 1 \\ \min \left\{ \phi \left( \varepsilon_{\text{Eve},M}^{\text{th}} \right), \phi \left( 1 - \frac{D_{\text{loss}} - \tilde{D}_{\text{Bob}}^{\text{th}}}{\alpha^0 D_{\text{loss}}} \right) \right\} & \text{if } \beta_2^{\text{Bob}} = 1 \\ \min \left\{ \phi \left( \varepsilon_{\text{Eve},M}^{\text{th}} \right), \phi \left( \frac{\tilde{D}_{\text{Bob}}^{\text{th}} - (1 - \alpha^0)D_{\text{conf}}}{D_{\text{loss}} - (1 - \alpha^0)D_{\text{conf}}} \right) \right\} & \text{if } \beta_3^{\text{Bob}} = 1, \end{cases} \quad (60)$$

$$n_K^{\min} = \begin{cases} n_K^{\min} = \phi \left[ \min \left( \varepsilon_{\text{Bob},K}^{\text{th}}, \frac{\tilde{D}_{\text{Bob}}^{\text{th}}}{\alpha^0 D_{\text{conf}}} \right) \right] & \text{if } \beta_1^{\text{Bob}} = 1 \\ \phi \left[ \min \left( \varepsilon_{\text{Bob},K}^{\text{th}}, \frac{\tilde{D}_{\text{Bob}}^{\text{th}} + (\alpha^0 - 1)D_{\text{loss}}}{\alpha^0 D_{\text{loss}}} \right) \right] & \text{if } \beta_2^{\text{Bob}} = 1 \\ \phi \left[ \min \left( \varepsilon_{\text{Bob},K}^{\text{th}}, \frac{\tilde{D}_{\text{Bob}}^{\text{th}} - (1 - \alpha^0)(\mathcal{S}-1)D_{\text{conf}}}{\alpha^0(\mathcal{S}-2)D_{\text{conf}}} \right) \right] & \text{if } \beta_3^{\text{Bob}} = 1. \end{cases} \quad (61)$$

Next, we investigate the monotonicity of the objective functions corresponding to *Eve's* three strategies to determine the optimal boundary point. Given the predicted strategy of *Bob*, the maximum value of  $\min \check{D}_{\text{Eve}}$  can be directly obtained using the corresponding computed boundary point.

#### 4) Optimal Point for *Eve's* Perception Strategy

If *Alice* predicts that *Eve* will select the *Perception*, i.e.,  $\beta_1^{\text{Eve}} = 1$ , the objective function (40a) becomes:

$$\check{D}_{\text{Eve}}^{\beta_1} = \varepsilon_{\text{Eve},M} D_{\text{loss}} + \alpha^0 (1 - \varepsilon_{\text{Eve},M}) \varepsilon_{\text{Eve},M} D_{\text{conf}}, \quad (62)$$

where the objective function is the same as (11). Thus, we can directly obtain the optimized resource allocation scheme from (33).

#### 5) Optimal Point for *Eve's* Dropping Strategy

If *Alice* predicts that *Eve* selects the strategy *Dropping*, i.e.,  $\beta_2^{\text{Eve}} = 1$ , the objective function (40a) becomes:

$$\begin{aligned} \check{D}_{\text{Eve}}^{\beta_2} = & \varepsilon_{\text{Eve},M} D_{\text{loss}} \\ & + (1 - \varepsilon_{\text{Eve},M}) [\varepsilon_{\text{Eve},K} \alpha^0 + (1 - \alpha^0)] D_{\text{loss}}. \end{aligned} \quad (63)$$

**Theorem 2.** If  $\beta_2^{\text{Eve}} = 1$ , the maximum of  $\check{D}_{\text{Eve}}^{\beta_2}$  is obtained at  $(n_M^{\min}, n_K^{\min})$ .

*Proof.* From (17) we can derive the monotonicity of  $\check{D}_{\text{Eve}}^{\beta_2}$  with respect to  $n_M$  and  $n_K$  respectively:

$$\frac{\partial \check{D}_{\text{Eve}}^{\beta_2}}{\partial n_K} = \frac{\partial \varepsilon_{\text{Eve},K}}{\partial n_K} \alpha^0 (1 - \varepsilon_{\text{Eve},M}) D_{\text{loss}} < 0, \quad (64)$$

$$\frac{\partial \check{D}_{\text{Eve}}^{\beta_2}}{\partial n_M} = \frac{\partial \varepsilon_{\text{Eve},M}}{\partial n_M} \alpha^0 (1 - \varepsilon_{\text{Eve},K}) D_{\text{loss}} < 0. \quad (65)$$

Thus,  $\check{D}_{\text{Eve}}^{\beta_2}$  is monotonically decreasing with respect to  $n_M$  and  $n_K$  respectively.  $\square$

Thus, the maximum of  $\check{D}_{\text{Eve}}^{\beta_2}$  can be formulated as:

$$\begin{aligned} \max \check{D}_{\text{Eve}}^{\beta_2} = & \varepsilon_{\text{Eve},M}^{\max} D_{\text{loss}} \\ & + (1 - \varepsilon_{\text{Eve},M}^{\max}) [\varepsilon_{\text{Eve},K} \alpha^0 + (1 - \alpha^0)] D_{\text{loss}}, \end{aligned} \quad (66)$$

where

$$\varepsilon_{\text{Eve},M}^{\max} = \mathcal{Q} \left( \sqrt{\frac{n_M^{\min}}{V_{\text{Eve}}}} \left( \mathcal{C}_{\text{Eve}} - \frac{d_M}{n_M^{\min}} \right) \ln 2 \right), \quad (67)$$

$$\varepsilon_{\text{Eve},K}^{\max} = \mathcal{Q} \left( \sqrt{\frac{n_K^{\min}}{V_{\text{Eve}}}} \left( \mathcal{C}_{\text{Eve}} - \frac{d_K}{n_K^{\min}} \right) \ln 2 \right). \quad (68)$$

The actual minimum values of  $n_M$  and  $n_K$  depend on *Alice's* prediction of *Bob*, as discussed above.

#### 6) Optimal Point for *Eve's* Exclusion Strategy

Finally, if *Alice* predicts that *Eve* will select strategy *Exclusion*, that is,  $\beta_3^{\text{Eve}} = 1$ , the objective function becomes as follows:

$$\begin{aligned} \check{D}_{\text{Eve}}^{\beta_3} = & \varepsilon_{\text{Eve},M} D_{\text{loss}} \\ & + (1 - \varepsilon_{\text{Eve},M}) \cdot \\ & \left[ \varepsilon_{\text{Eve},K} \frac{\alpha^0(\mathcal{S}-2)}{\mathcal{S}-1} D_{\text{conf}} + (1 - \alpha^0) D_{\text{conf}} \right]. \end{aligned} \quad (69)$$

**Theorem 3.** If  $\beta_3^{\text{Eve}} = 1$ , the maximum of  $\check{D}_{\text{Eve}}^{\beta_3}$  is obtained at  $(n_M^{\max}, n_K^{\min})$  when  $\alpha^0 < \frac{D_{\text{conf}} - D_{\text{loss}}}{D_{\text{conf}}(1 - \varepsilon_{\text{Eve},K}^{\max}) \frac{\mathcal{S}-2}{\mathcal{S}-1}}$ , while achieved at  $(n_M^{\min}, n_K^{\min})$  when  $\alpha^0 \geq \frac{D_{\text{conf}} - D_{\text{loss}}}{D_{\text{conf}}(1 - \varepsilon_{\text{Eve},K}^{\max}) \frac{\mathcal{S}-2}{\mathcal{S}-1}}$ .

*Proof.* We first calculate the first-order derivatives of  $\check{D}_{\text{Eve}}^{\beta_3}$  with respect to  $n_M$  and  $n_K$  respectively:

$$\begin{aligned} \frac{\partial \check{D}_{\text{Eve}}^{\beta_3}}{\partial n_M} &= \frac{\partial \varepsilon_{\text{Eve},M}}{\partial n_M} [D_{\text{loss}} - D_{\text{conf}} \\ &\quad + \alpha^o D_{\text{conf}} (1 - \varepsilon_{\text{Eve},K} \frac{\mathcal{S} - 2}{\mathcal{S} - 1})] \end{aligned} \quad (70)$$

$$\frac{\partial \check{D}_{\text{Eve}}^{\beta_3}}{\partial n_K} = \frac{\partial \varepsilon_{\text{Eve},K}}{\partial n_K} (1 - \varepsilon_{\text{Eve},M}) \frac{\alpha^o (\mathcal{S} - 2)}{\mathcal{S} - 1} D_{\text{conf}} < 0. \quad (71)$$

From the above equations, we can conclude that  $\check{D}_{\text{Eve}}^{\beta_3}$  is monotonically decreasing with respect to  $n_K$ , while the monotonicity of  $\check{D}_{\text{Eve}}^{\beta_3}$  with respect to  $n_M$  depends on the value of  $\alpha^o$ . When  $\alpha^o < \frac{D_{\text{conf}} - D_{\text{loss}}}{D_{\text{conf}} (1 - \varepsilon_{\text{Eve},K} \frac{\mathcal{S} - 2}{\mathcal{S} - 1})}$ , we can derive

that  $\frac{\partial \check{D}_{\text{Eve}}^{\beta_3}}{\partial n_M} > 0$ , which means that  $\check{D}_{\text{Eve}}^{\beta_3}$  is monotonically increasing with respect to  $n_M$ . In this case, the optimum must be obtained at  $(n_M^{\max}, n_K^{\min})$ .

On the other hand, when  $\alpha^o \geq \frac{D_{\text{conf}} - D_{\text{loss}}}{D_{\text{conf}} (1 - \varepsilon_{\text{Eve},K} \frac{\mathcal{S} - 2}{\mathcal{S} - 1})}$ , we can derive that  $\frac{\partial \check{D}_{\text{Eve}}^{\beta_3}}{\partial n_M} \leq 0$ , which means that  $\check{D}_{\text{Eve}}^{\beta_3}$  is decreasing with respect to  $n_M$ . So the optimum is located at  $(n_M^{\min}, n_K^{\min})$  in this case.  $\square$

#### D. Optimization Algorithm

---

##### Algorithm 1: Optimization of $n_M$ , $n_K$ and $\alpha^o$

---

```

1 Input:  $T$ ,  $\tilde{D}_{\text{Bob}}^{\text{th}}$ ,  $\varepsilon_{\text{Bob},M}$ ,  $\varepsilon_{\text{Bob},K}$ ,  $\mathbb{E}\{\varepsilon_{\text{Eve},M}\}$ ,  $\mathbb{E}\{\varepsilon_{\text{Eve},K}\}$ 
2 Initialize:  $n_M = n_M^{\text{init}}$ ,  $n_K = n_K^{\text{init}}$ ,  $\alpha = \alpha^{\text{init}}$ ,
 $\beta_1^{\text{Bob}} = 1$ ,  $\beta_2^{\text{Bob}} = 0$ ,  $\beta_3^{\text{Bob}} = 0$ ,  $\beta_1^{\text{Eve}} = 1$ ,  $\beta_2^{\text{Eve}} = 0$ ,
 $\beta_3^{\text{Eve}} = 0$ ,
3 where  $n_M^{\text{init}} = \min \left\{ \phi \left( \varepsilon_{\text{Eve},M}^{\text{th}} \right), \phi \left( \frac{\tilde{D}_{\text{Bob}}^{\text{th}}}{D_{\text{loss}}} \right) \right\}$ ,
 $n_K^{\text{init}} = \phi \left[ \min \left( \varepsilon_{\text{Bob},K}^{\text{th}}, \frac{\tilde{D}_{\text{Bob}}^{\text{th}}}{\alpha^{\text{init}} D_{\text{conf}}} \right) \right]$ 
4 do
5    $(\beta_1^{\text{Eve}(t)}, \beta_2^{\text{Eve}(t)}, \beta_3^{\text{Eve}(t)}) \leftarrow$ 
    $\arg \min_{\beta_1, \beta_2, \beta_3} \tilde{D}_{\text{Eve}}(n_M^{(t-1)}, n_K^{(t-1)})$ ,
6    $(\beta_1^{\text{Bob}(t)}, \beta_2^{\text{Bob}(t)}, \beta_3^{\text{Bob}(t)}) \leftarrow$ 
    $\arg \min_{\beta_1, \beta_2, \beta_3} \tilde{D}_{\text{Bob}}(n_M^{(t-1)}, n_K^{(t-1)})$ 
7    $\min \tilde{D}_{\text{Eve}}^{(t)} := \tilde{D}_{\text{Eve}}(\beta_1^{\text{Eve}(t)}, \beta_2^{\text{Eve}(t)}, \beta_3^{\text{Eve}(t)})$ 
8    $\min \tilde{D}_{\text{Bob}}^{(t)} := \tilde{D}_{\text{Bob}}(\beta_1^{\text{Bob}(t)}, \beta_2^{\text{Bob}(t)}, \beta_3^{\text{Bob}(t)})$ 
9    $\alpha^{o(t)} \leftarrow \arg \max_{\alpha} \left[ \min \tilde{D}_{\text{Eve}}^{(t)} \right]$ 
10   $(n_M^{(t)}, n_K^{(t)}) \leftarrow \arg \max_{n_M, n_K} \left[ \min \tilde{D}_{\text{Eve}}^{(t)}(\alpha^{o(t)}) \right]$ 
11   $t \leftarrow t + 1$ 
12 while  $t \leq T$ ;
13 return  $n_M$ ,  $n_K$  and  $\alpha^o$ 

```

---

Based on the above theoretical analysis, we propose the following algorithm 1 to optimize the resource allocation process and encryption process. In the first step, we set an initial value for the encryption rate  $\alpha$ . Since *Alice* cannot yet predict the decryption strategies of *Bob* and *Eve*, we assume by default that both *Bob* and *Eve* adopt the *Perception* strategy. It is important to note that this assumption does not affect the

periodicity of the subsequent iterative optimization process or the predicted selection of *Eve*'s decryption strategy in each iteration. We have verified this through simulation. Under our specified simulation parameters, altering *Eve*'s initial strategy selection always results in a regression to the *Dropping* strategy by the second iteration. Furthermore, *Alice* predicts *Eve*'s behavior under a worst-case assumption, wherein *Eve* is assumed to have complete knowledge of *Alice*'s resource allocation scheme and deceptive encryption probability. If *Eve* deviates from the proposed decryption mechanism and arbitrarily selects a decryption strategy rather than one that minimizes her own semantic distortion, she will inevitably experience greater losses. Based on this assumption, the initial  $(n_M^{\text{init}}, n_K^{\text{init}})$  is calculated using equation (27) and (32).

Subsequently, *Alice* calculates the distortion for *Eve* and *Bob* under the three strategies according to equation (13), and selects the one that yields the minimum distortion as the predicted decryption strategy for *Eve* and *Bob*. Based on *Alice*'s predicted strategies  $(\beta_1^{\text{Eve}(t)}, \beta_2^{\text{Eve}(t)}, \beta_3^{\text{Eve}(t)})$  and  $(\beta_1^{\text{Bob}(t)}, \beta_2^{\text{Bob}(t)}, \beta_3^{\text{Bob}(t)})$ , *Alice* adjusts the encryption rate  $\alpha$  to maximize *Eve*'s distortion while ensuring that *Bob*'s distortion remains at a low level. The optimal value of  $\alpha$  depends on *Alice*'s predicted strategies for *Eve* and *Bob*, with the computation processes given in (38) and (39). After determining the optimal  $\alpha^{o(t)}$ , *Alice* can reallocate the resources. Based on the previous predictions for *Eve* and *Bob*, the new  $(n_M^{(t)}, n_K^{(t)})$  can be calculated using (60) and (61). During the iteration process, *Alice*'s predicted strategies for *Eve* and *Bob* change continuously with variations in  $\alpha$  and the coding rate, making it difficult to ensure the convergence of the distortion. Therefore, we set a maximum number of iterations  $T$ , and the loop is terminated once the iteration count exceeds  $T$ . Since the optimal values can be computed analytically, the computational complexity of the algorithm is proportional to the number of iterations, i.e.,  $\mathcal{O}(T)$ . Compared with our previous work that employed the deception rate as the objective function [9], the proposed algorithm, which adopts semantic distortion as the optimization criterion, significantly reduces the computational complexity.

## V. NUMERICAL EVALUATION

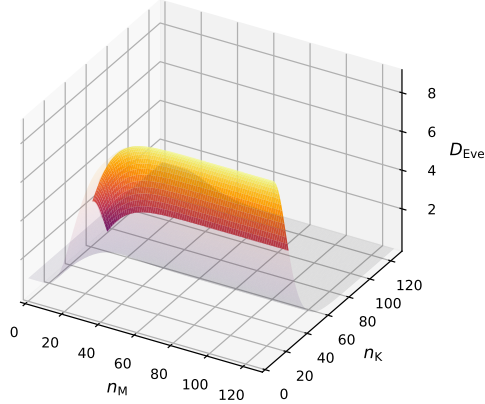
To verify our theoretical analysis and to examine the effectiveness of our proposed optimization algorithm, we conducted a series of simulation experiments. The simulation parameters are listed in Table I, while the specific parameters for each task will be presented later.

### A. Semantic Distortion Surface

To verify the convexity of the Problem (40), we plot the corresponding surface of  $\min \tilde{D}_{\text{Eve}}$  in the region of  $(n_M, n_K) \in \{1, 2, \dots, 128\} \times \{1, 2, \dots, 128\}$ , as shown in Fig. 6. It is worth noting that the objective function and constraints vary depending on the strategies chosen by *Eve* and *Bob*, resulting in a total of  $3 \times 3$  theoretical cases. In the theoretical analysis section, all 9 cases are thoroughly discussed. In the simulation section, we present only one representative case as an example, in which both *Eve* and *Bob* adopt the *Perception*

TABLE I: Simulation setup

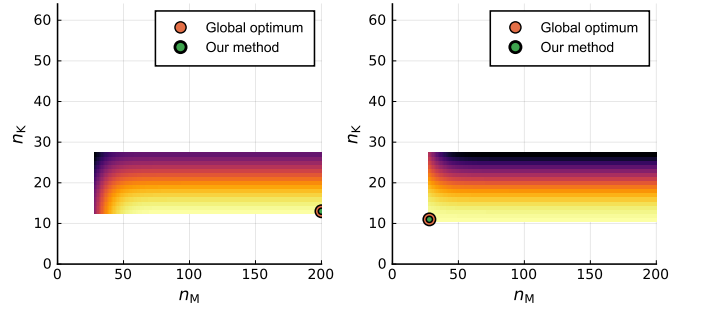
Parameter	Value	Remark
$\sigma^2$	1 mW	Noise power
$B$	1 Hz	Normalized to unity bandwidth
$d_M$	16 bits	Length of ciphertext
$d_K$	16 bits	Length of key
$D_{\text{loss}}$	1	Distortion between plaintext and ciphertext
$D_{\text{conf}}$	10	Distortion between plaintext and invalid decoding codeword
$\varepsilon_{\text{Bob},M}^{\text{th}}$		
$\varepsilon_{\text{Bob},K}^{\text{th}}$	0.5	Thresholds in constraints (16c)–(16f)
$\varepsilon_{\text{Eve},M}^{\text{th}}$		
$\varepsilon_{\text{Eve},K}^{\text{th}}$		
$\tilde{D}_{\text{Bob}}^{\text{th}}$	0.01	Threshold in constraints (40c)
$T$	100	Maximum number of simulation iterations

Fig. 6: Semantic distortion with  $\alpha = 0.9$ .

strategy. We set the legitimate channel gain  $z_{\text{Bob}} = 0 \text{ dB}$ , the eavesdropping channel gain  $z_{\text{Eve}} = -10 \text{ dB}$ , and the encryption rate  $\alpha = 0.9$ . The feasible region defined by constraints (40b)–(40c) is displayed with higher opacity compared to the rest of the surface, and lighter colors indicate larger distortion values. As illustrated in the figure, the surface is concave, with distortion decreasing monotonically with  $n_K$  and increasing monotonically with  $n_M$ . This result is consistent with our analysis regarding the monotonicity behavior when  $\alpha \geq \frac{D_{\text{loss}}}{\varepsilon_{\text{Eve},K}^{\max} D_{\text{conf}}}$ .

### B. Validation of the Proposed Algorithm

We continue to assume that both *Eve* and *Bob* adopt the perception strategy, set  $h_{\text{Eve}} = -10 \text{ dB}$  and  $h_{\text{Bob}} = 0 \text{ dB}$ , while vary the value of  $\alpha$ . According to our theoretical analysis, when  $\alpha \geq \frac{D_{\text{loss}}}{\varepsilon_{\text{Eve},K}^{\max} D_{\text{conf}}}$ ,  $D_{\text{Eve}}$  increases monotonically with  $n_M$ , and the optimal value is achieved at  $(n_K^{\min}, n_M^{\max})$ . Conversely, when  $\alpha < \frac{D_{\text{loss}}}{\varepsilon_{\text{Eve},K}^{\max} D_{\text{conf}}}$ ,  $D_{\text{Eve}}$  decreases monotonically with  $n_M$ , and the optimum occurs at  $(n_K^{\min}, n_M^{\min})$ . Therefore, we set  $\alpha = 0.9$  and  $\alpha = 0.1$ , respectively, and plot the feasible region along with the corresponding optimal values. As illustrated in Fig. 7, the value of  $\alpha$  influences the

Fig. 7: Global optimum in the feasible region with  $\alpha = 0.9$  (left) and  $\alpha = 0.1$  (right).

monotonic behavior of  $D_{\text{Eve}}$ , which is consistent with our theoretical analysis.

In addition, according to our proposed method, the optimal  $(n_M, n_K)$  can be determined by analyzing the monotonicity of the objective function  $\min \tilde{D}_{\text{Eve}}$  and computing the boundary points based on the constraints (40b)–(40c). The Fig. 7 shows that the boundary of the feasible region is rectangular, and by directly calculating the boundary points, the global optimum can be efficiently identified.

### C. Optimization of Resource Allocation and Encryption Rate

According to Algorithm 1,  $n_M$ ,  $n_K$ , and  $\alpha$  can be updated iteratively. To investigate the convergence of the algorithm, we set the maximum number of iterations  $T = 100$ , with  $h_{\text{Eve}} = 0 \text{ dB}$  and  $h_{\text{Bob}} = 5 \text{ dB}$ . We then plot the most likely strategies chosen by *Eve* and *Bob* at each iteration, along with their corresponding distortion values, to observe the underlying patterns.

We first set the cardinality of the codebook to its minimum, i.e.,  $\mathcal{S} = 2$ . In the initial iteration, we assume  $\alpha = 0.9$  and that both *Eve* and *Bob* adopt the perception strategy. Note that we consider the worst-case scenario in which both *Bob* and *Eve* possess full knowledge of *Alice*'s resource allocation and encryption strategies—specifically, the parameters  $(n_M, n_K)$  and  $\alpha$ . Once the CSI of their respective channels is available, they can evaluate the semantic distortion associated with each of the three strategies using (13). In the event of a key decoding failure, they will select the strategy that minimizes their individual distortion.

Similarly, from *Alice*'s perspective, once the CSI for legitimate and the statistical expectation of CSI for eavesdropping channels are available, it can calculate the distortion of each strategy according to (13). Thus, it can anticipate the decryption strategies that *Bob* and *Eve* are likely to adopt under the previous parameters  $(n_M^{(t-1)}, n_K^{(t-1)})$  and  $\alpha^{o(t-1)}$ . In the  $t$ -th iteration, *Alice* employs (37) and (40) to minimize the distortion of the predicted scheme of *Eve*, thereby obtaining updated values for  $(n_M^{(t)}, n_K^{(t)})$  and  $\alpha^{o(t)}$ . Following this update, both the coding rate and the encryption strategy are modified, which in turn alters the distortions associated with the three strategies. Consequently, the decryption strategies selected by *Bob* and *Eve* may also change in the next iteration.

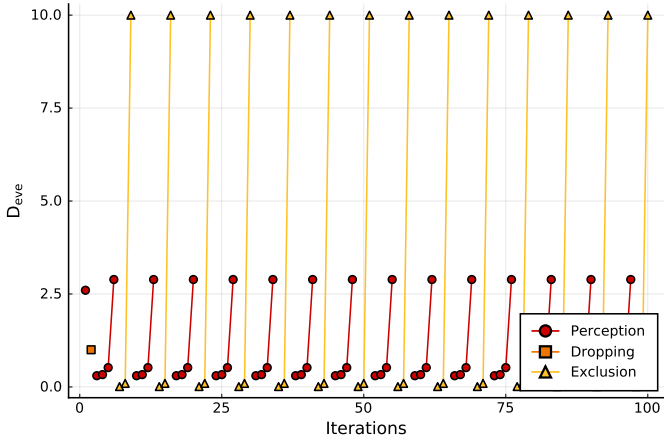


Fig. 8:  $D_{\text{Eve}}$  for different decryption strategies with  $\mathcal{S} = 2$ ,  $h_{\text{Eve}} = 0 \text{ dB}$ ,  $h_{\text{Bob}} = 5 \text{ dB}$ .

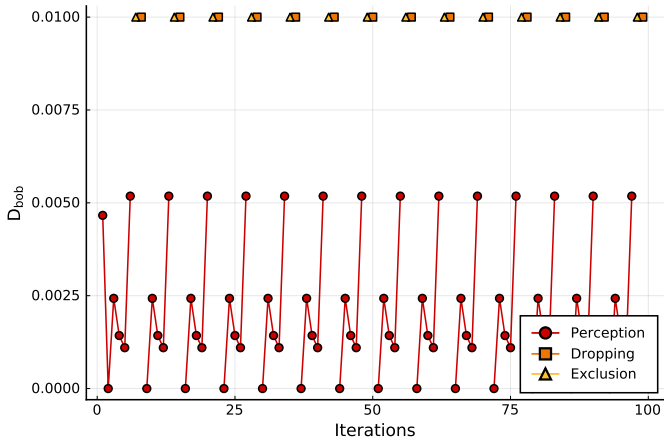


Fig. 9:  $D_{\text{Bob}}$  for different decryption strategies with  $\mathcal{S} = 2$ ,  $h_{\text{Eve}} = 0 \text{ dB}$ ,  $h_{\text{Bob}} = 5 \text{ dB}$ .

Therefore, in each subsequent iteration after initiation, the strategies of *Eve* and *Bob* are re-estimated, and  $\alpha$ ,  $n_M$ , and  $n_K$  are updated based on the new objective function. The simulation results are shown in Fig. 8 and Fig. 9. As the iterations progress, the distortion values for *Eve* and *Bob* do not converge to constant values, but rather fluctuate according to the changes in their likely chosen strategies, which is also consistent with our theoretical analysis. The selected strategies and the corresponding distortion values exhibit a periodic pattern. When  $\mathcal{S} = 2$ , due to the small codebook cardinality, *Eve* tends to prefer the *Exclusion* strategy. In contrast, *Bob* mostly selects the perception strategy, as the legitimate channel generally has better conditions.

Next, we set the codebook cardinality to its maximum value, i.e.,  $\mathcal{S} = 2^{16}$ . The simulation results are shown in Fig. 10 and Fig. 11. Similarly, the strategies that *Eve* and *Bob* are likely to choose exhibit a periodic pattern. Compared to the case when  $\mathcal{S} = 2$ , neither *Eve* nor *Bob* chooses the exclusion strategy.

## VI. CONCLUSION

In this work, we extend the PLD framework based on semantic communication by explicitly incorporating the re-

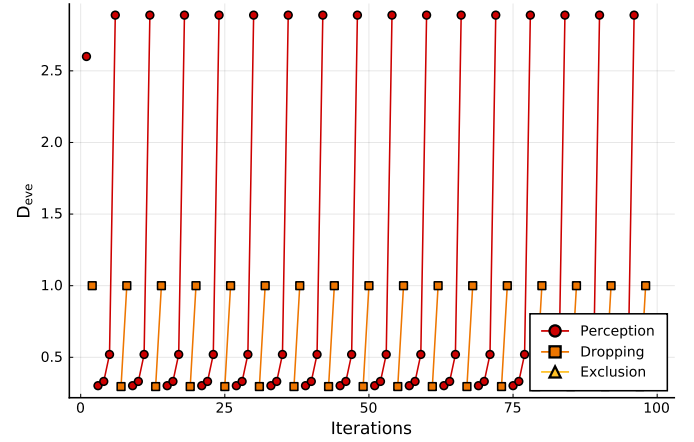


Fig. 10:  $D_{\text{Eve}}$  for different decryption strategies with  $\mathcal{S} = 2^{16}$ ,  $h_{\text{Eve}} = 0 \text{ dB}$ ,  $h_{\text{Bob}} = 5 \text{ dB}$ .

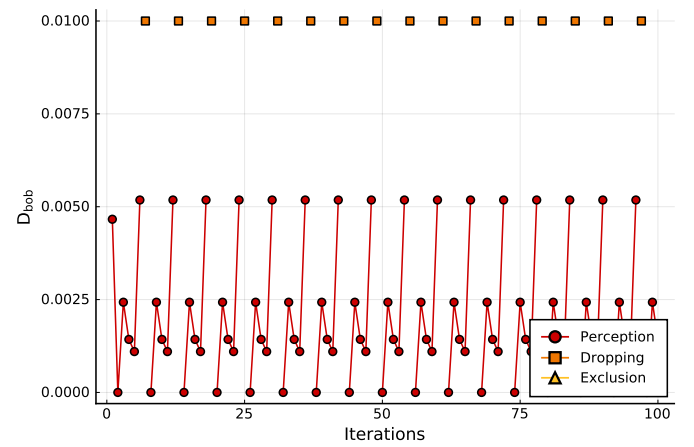


Fig. 11:  $D_{\text{Bob}}$  for different decryption strategies with  $\mathcal{S} = 2^{16}$ ,  $h_{\text{Eve}} = 0 \text{ dB}$ ,  $h_{\text{Bob}} = 5 \text{ dB}$ .

ceiver's decryption strategies into the optimization of *Alice*'s encryption policy. Specifically, when key decryption fails, the receiver may adopt one of three strategies: directly interpreting the ciphertext as plaintext, discarding the information, or selecting a most likely candidate from the codebook. Given the CSI of the legitimate channel and the statistical expectations of the CSI of the eavesdropping channel, *Alice* can evaluate the semantic distortion corresponding to each strategy and thereby anticipate the receiver's likely choice. In this case, *Alice* iteratively optimizes the code lengths ( $n_M, n_K$ ) and the encryption probability  $\alpha$  with the objective of maximizing *Eve*'s semantic distortion. This ensures that *Eve* is more likely to lose information or be misled, thus enabling active counteract against eavesdropping. The joint selection of decryption strategies by *Bob* and *Eve* leads to nine possible cases. We analyze each case in detail and derive closed-form expressions for the optimal solutions. Furthermore, numerical simulations are conducted to validate the concavity of the objective function and to confirm the practicality of the proposed optimization algorithm. Our results reveal that the optimal values exhibit a periodic pattern under iterative optimization. Due to the

superior channel conditions, *Bob* tends to adopt the *Perception* strategy, while *Eve*, particularly when the codebook cardinality is small, is more inclined to select the *Exclusion* strategy. Through the proposed optimization scheme, *Alice* is able to maximize *Eve*'s semantic distortion effectively.

## REFERENCES

- [1] J. M. Hamamreh, H. M. Furqan, and H. Arslan, "Classifications and applications of physical layer security techniques for confidentiality: A comprehensive survey," *IEEE Communications Surveys & Tutorials*, vol. 21, no. 2, pp. 1773–1828, 2018.
- [2] Y. Liu, H.-H. Chen, and L. Wang, "Physical layer security for next generation wireless networks: Theories, technologies, and challenges," *IEEE Communications Surveys & Tutorials*, vol. 19, no. 1, pp. 347–376, 2017.
- [3] M. Mitev, A. Chorti, H. V. Poor, and G. P. Fettweis, "What physical layer security can do for 6G security," *IEEE Open Journal of Vehicular Technology*, vol. 4, pp. 375–388, 2023.
- [4] A. Chaman, J. Wang, J. Sun, H. Hassanieh, and R. Roy Choudhury, "Ghostbuster: Detecting the presence of hidden eavesdroppers," in *Proceedings of the 24th annual international conference on mobile computing and networking*, 2018, pp. 337–351.
- [5] X. Zhou, R. K. Ganti, J. G. Andrews, and A. Hjorungnes, "On the throughput cost of physical layer security in decentralized wireless networks," *IEEE Transactions on Wireless Communications*, vol. 10, no. 8, pp. 2764–2775, 2011.
- [6] D. Wang, B. Bai, W. Zhao, and Z. Han, "A survey of optimization approaches for wireless physical layer security," *IEEE Communications Surveys & Tutorials*, vol. 21, no. 2, pp. 1878–1911, 2018.
- [7] C. Wang and Z. Lu, "Cyber deception: Overview and the road ahead," *IEEE Security & Privacy*, vol. 16, no. 2, pp. 80–85, 2018.
- [8] B. Han, Y. Zhu, A. Schmeink, and H. D. Schotten, "Non-orthogonal multiplexing in the FBL regime enhances physical layer security with deception," in *2023 IEEE 24th International Workshop on Signal Processing Advances in Wireless Communications (SPAWC)*. IEEE, 2023, pp. 211–215.
- [9] W. Chen, B. Han, Y. Zhu, A. Schmeink, G. Caire, and H. D. Schotten, "Physical layer deception with non-orthogonal multiplexing," *IEEE Transactions on Wireless Communications*, 2025.
- [10] W. Chen, B. Han, Y. Zhu, A. Schmeink, and H. D. Schotten, "Physical layer deception in OFDM systems," in *2025 Joint European Conference on Networks and Communications & 6G Summit (EuCNC/6G Summit)*, 06 2025, pp. 715–720.
- [11] B. Han, Y. Zhu, A. Schmeink, G. Caire, and H. D. Schotten, "A semantic model for physical layer deception," in *ICC 2025 - IEEE International Conference on Communications*, 2025, pp. 4129–4134.
- [12] C. E. Shannon, "Communication theory of secrecy systems," *The Bell System Technical Journal*, vol. 28, no. 4, pp. 656–715, 1949.
- [13] A. D. Wyner, "The wire-tap channel," *The Bell System Technical Journal*, vol. 54, no. 8, pp. 1355–1387, 1975.
- [14] I. Csiszár and J. Körner, "Broadcast channels with confidential messages," *IEEE transactions on information theory*, vol. 24, no. 3, pp. 339–348, 2003.
- [15] S. Leung-Yan-Cheong and M. Hellman, "The gaussian wire-tap channel," *IEEE Transactions on Information Theory*, vol. 24, no. 4, pp. 451–456, 1978.
- [16] J. Barros and M. R. Rodrigues, "Secrecy capacity of wireless channels," in *2006 IEEE international symposium on information theory*. IEEE, 2006, pp. 356–360.
- [17] A. O. Hero, "Secure space-time communication," *IEEE Transactions on Information Theory*, vol. 49, no. 12, pp. 3235–3249, 2004.
- [18] P. Parada and R. Blahut, "Secrecy capacity of simo and slow fading channels," in *Proceedings. International Symposium on Information Theory, 2005. ISIT 2005*. IEEE, 2005, pp. 2152–2155.
- [19] Z. Li, W. Trappe, and R. Yates, "Secret communication via multi-antenna transmission," in *2007 41st Annual Conference on Information Sciences and Systems*. IEEE, 2007, pp. 905–910.
- [20] Y. Liang, H. V. Poor, and S. Shamai, "Secure communication over fading channels," *IEEE Transactions on Information Theory*, vol. 54, no. 6, pp. 2470–2492, 2008.
- [21] R. Liu, I. Maric, R. D. Yates, and P. Spasojevic, "The discrete memoryless multiple access channel with confidential messages," in *2006 IEEE International Symposium on Information Theory*. IEEE, 2006, pp. 957–961.
- [22] Y. Liang, A. Somekh-Baruch, H. V. Poor, S. Shamai, and S. Verdú, "Capacity of cognitive interference channels with and without secrecy," *IEEE Transactions on Information Theory*, vol. 55, no. 2, pp. 604–619, 2009.
- [23] Y. Oohama, "Capacity theorems for relay channels with confidential messages," in *2007 IEEE International Symposium on Information Theory*. IEEE, 2007, pp. 926–930.
- [24] M. Bloch, J. Barros, M. R. D. Rodrigues, and S. W. McLaughlin, "Wireless information-theoretic security," *IEEE Transactions on Information Theory*, vol. 54, no. 6, pp. 2515–2534, 2008.
- [25] Q. Li and W.-K. Ma, "Spatially selective artificial-noise aided transmit optimization for MISO multi-eves secrecy rate maximization," *IEEE Transactions on Signal Processing*, vol. 61, no. 10, pp. 2704–2717, 2013.
- [26] A. Khisti and G. W. Wornell, "Secure transmission with multiple antennas I: The MISOME wiretap channel," *IEEE Transactions on Information Theory*, vol. 56, no. 7, pp. 3088–3104, 2010.
- [27] D. Wang, B. Bai, W. Zhao, and Z. Han, "A survey of optimization approaches for wireless physical layer security," *IEEE Communications Surveys & Tutorials*, vol. 21, no. 2, pp. 1878–1911, 2019.
- [28] Y. Polyanskiy, H. V. Poor, and S. Verdú, "Channel coding rate in the finite blocklength regime," *IEEE Transactions on Information Theory*, vol. 56, no. 5, pp. 2307–2359, 2010.
- [29] B. Liu, P. Zhu, J. Li, D. Wang, and X. You, "Energy-efficient optimization in distributed massive mimo systems for slicing eMBB and uRLLC services," *IEEE Transactions on Vehicular Technology*, vol. 72, no. 8, pp. 10473–10487, 2023.
- [30] T. Li, H. Zhang, J. Qiao, and J. Tian, "Robust beamforming design with finite blocklength for uRLLC," *IEEE Transactions on Vehicular Technology*, vol. 72, no. 2, pp. 2604–2608, 2023.
- [31] M. Soleymani, I. Santamaria, E. A. Jorswieck, R. Schober, and L. Hanzo, "Optimization of the downlink spectral- and energy- efficiency of riser-aided multi-user uRLLC mimo systems," *IEEE Transactions on Communications*, vol. 73, no. 5, pp. 3497–3513, 2025.
- [32] W. Yang, R. F. Schaefer, and H. V. Poor, "Wiretap channels: Nonasymptotic fundamental limits," *IEEE Transactions on Information Theory*, vol. 65, no. 7, pp. 4069–4093, 2019.
- [33] C. Wang, Z. Li, H. Zhang, D. W. K. Ng, and N. Al-Dhahir, "Achieving covertness and security in broadcast channels with finite blocklength," *IEEE Transactions on Wireless Communications*, vol. 21, no. 9, pp. 7624–7640, 2022.
- [34] M. Oh, J. Park, and J. Choi, "Joint optimization for secure and reliable communications in finite blocklength regime," *IEEE Transactions on Wireless Communications*, vol. 22, no. 12, pp. 9457–9472, 2023.
- [35] Y. Zhu, X. Yuan, Y. Hu, R. F. Schaefer, and A. Schmeink, "Trade reliability for security: Leakage-failure probability minimization for machine-type communications in uRLLC," *IEEE Journal on Selected Areas in Communications*, vol. 41, no. 7, pp. 2123–2137, 2023.
- [36] B. Cheswick, "An evening with berferd in which a cracker is lured, endured, and studied," in *Proc. Winter USENIX Conference, San Francisco*, 1992, pp. 20–24.
- [37] C. Stoll, *The cuckoo's egg: tracking a spy through the maze of computer espionage*. Simon and Schuster, 2024.
- [38] D. Fraunholz, S. D. Anton, C. Lipps, D. Reti, D. Krohmer, F. Pohl, M. Tammen, and H. D. Schotten, "Demystifying deception technology: A survey," *arXiv preprint arXiv:1804.06196*, 2018.
- [39] X. Han, N. Kheir, and D. Balzarotti, "Deception techniques in computer security: A research perspective," *ACM Comput. Surv.*, vol. 51, no. 4, pp. 1–36, 2018.
- [40] J. Pawlick, E. Colbert, and Q. Zhu, "A game-theoretic taxonomy and survey of defensive deception for cybersecurity and privacy," *ACM Comput. Surv.*, vol. 52, no. 4, pp. 1–28, 2019.
- [41] Q. He, S. Fang, T. Wang, Y. Liu, S. Zhao, and Z. Lu, "Proactive anti-eavesdropping with trap deployment in wireless networks," *IEEE Transactions on Dependable and Secure Computing*, vol. 20, no. 1, pp. 637–649, 2023.
- [42] P. Qi, Y. Meng, S. Zheng, X. Zhou, N. Cheng, and Z. Li, "Adversarial defense embedded waveform design for reliable communication in the physical layer," *IEEE Internet of Things Journal*, vol. 11, no. 10, pp. 18136–18153, 2024.
- [43] N. Ye, J. Liu, J. Pan, Y. Xiang, B. Qi, C. Liu, X. Li, and S. Mumtaz, "Anti-interception countermeasure for air-space-ground-maritime integrated networks: From signal concealment to defensive deception," *IEEE Communications Magazine*, vol. 63, no. 7, pp. 64–71, 2025.
- [44] Y. Shao, Q. Cao, and D. Gündüz, "A theory of semantic communication," *IEEE Transactions on Mobile Computing*, vol. 23, no. 12, pp. 12211–12228, 2024.